

1 **Assembly of D1/D2 complexes of photosystem II: binding of pigments and a** 2 **network of auxiliary proteins**

3 Jana Knoppová^a, Roman Sobotka^a, Jianfeng Yu^b, Martina Bečková^a, Jan Pilný^a, Joko P.
4 Trinugroho^b, Ladislav Csefalvay^a, David Bína^{c,d}, Peter J. Nixon^b, and Josef Komenda^{a,1}

5
6 ^aInstitute of Microbiology of the Czech Academy of Sciences, Centre Algatech, Laboratory of
7 Photosynthesis, 37901 Třeboň, Czech Republic; ^bSir Ernst Chain Building-Wolfson Laboratories,
8 Department of Life Sciences, Imperial College London, South Kensington Campus, London,
9 SW7 2AZ, UK; ^cFaculty of Science, University of South Bohemia in České Budějovice, 370 05,
10 České Budějovice, Czech Republic; ^dInstitute of Plant Molecular Biology, Biology Centre of the
11 Czech Academy of Sciences, 370 05, České Budějovice, Czech Republic.

12
13 ¹To whom correspondence should be addressed. E-mail: komenda@alga.cz

14
15 The author responsible for distribution of materials integral to the findings presented in this
16 article in accordance with the policy described in the Instructions for Authors
17 (<https://academic.oup.com/plphys/pages/General-Instructions>) is Josef Komenda.

18
19 **Running title:** Earliest steps in PSII assembly

20
21 **One sentence summary:** Analysis of isolated assembly complexes provides new insights into
22 the early stages of photosystem II biogenesis.

23 **Author contributions**

24 J.Kno and M.B. constructed strains and performed isolation of complexes and their
25 electrophoretic analyses; R.S. analyzed data and calculated pigment ratios; J.P. performed HPLC
26 pigment analyses; L.C. performed MS analyses of proteins; J.Y. and J.P.T. constructed strains
27 expressing tagged D1 and D2 proteins; D.B. measured charge separation activity; J.K. made
28 spectroscopic measurements and analysed electrophoretic and MS data; J.Kno., R.S., J.K., and
29 P.J.N. wrote the article; P.J.N. and J.K. acquired the funding and supervised the project; all
30 authors discussed the results and commented on the article.
31

32 **ABSTRACT**

33 Photosystem II (PSII) is the multi-subunit light-driven oxidoreductase that drives photosynthetic
34 electron transport using electrons extracted from water. To investigate the initial steps of PSII
35 assembly, we used strains of the cyanobacterium *Synechocystis* sp. PCC 6803 arrested at early
36 stages of PSII biogenesis and expressing affinity-tagged PSII subunits to isolate PSII reaction
37 center assembly (RCII) complexes and their precursor D1 and D2 modules (D1_{mod} and D2_{mod}).
38 RCII preparations isolated using either a His-tagged D2 or a FLAG-tagged PsbI subunit
39 contained the previously described RCIIa and RCII* complexes that differ with respect to the
40 presence of the Ycf39 assembly factor and high-light-inducible proteins (Hlips) and a larger
41 complex consisting of RCIIa bound to monomeric PSI. All RCII complexes contained the PSII
42 subunits D1, D2, PsbI, PsbE, and PsbF and the assembly factors rubredoxin A (RubA) and
43 Ycf48, but we also detected PsbN, Slr1470, and the Slr0575 proteins, which all have plant
44 homologs. The RCII preparations also contained prohibitins/stomatins (Phbs) of unknown
45 function and FtsH protease subunits. RCII complexes were active in light-induced primary charge
46 separation and bound chlorophylls, pheophytins, beta-carotenes, and heme. The isolated D1_{mod}
47 consisted of D1/PsbI/Ycf48 with some Ycf39 and Phb3, while D2_{mod} contained D2/cytochrome
48 b₅₅₉ with co-purifying PsbY, Phb1, Phb3, FtsH2/FtsH3, CyanoP, and Slr1470. As stably bound
49 chlorophyll was detected in D1_{mod} but not D2_{mod}, formation of RCII appears to be important for
50 stable binding of most of the chlorophylls and both pheophytins. We suggest that chlorophyll can
51 be delivered to RCII from either monomeric PSI or Ycf39/Hlip complexes.

52
53 **Keywords:** photosystem II biogenesis, reaction center assembly complex, assembly factors,
54 pigment binding

55

56 INTRODUCTION

57 Photosystem II (PSII) is the unique multi-subunit oxidoreductase embedded in the thylakoid
58 membranes (TM) of cyanobacteria and chloroplasts that catalyzes the solar-powered oxidation of
59 water. Electrons extracted from water are utilized for fixation of carbon into organic molecules
60 while molecular oxygen, the by-product of PSII activity, is released into the atmosphere. In
61 cyanobacteria, PSII consists of 17 intrinsic and three extrinsic protein subunits and numerous
62 pigments and redox-active cofactors (Zouni et al., 2001; Umena et al., 2011). At the heart of PSII
63 is a heterodimer of two homologous proteins, D1 and D2, both having five transmembrane
64 helices, which are flanked by two large chlorophyll (Chl) - binding inner antennae, known as
65 CP43 and CP47. There are also several low molecular mass (LMM) subunits which are rather
66 featureless except for PsbE and PsbF which bind heme to form cytochrome *b*₅₅₉ (Cyt *b*₅₅₉)
67 (Barber, 2014). The extrinsic luminal subunits PsbO, PsbU, PsbV, and CyanoQ serve to stabilize
68 the oxygen-evolving Mn₄CaO₅ cluster. In chloroplasts of plants and green algae, the luminal
69 PsbU and PsbV subunits have been replaced by the structurally different PsbP and PsbQ proteins,
70 while the intrinsic part of PSII is similar to that of cyanobacteria (Ifuku, 2015; Roose et al.,
71 2016).

72 Biogenesis of this complicated molecular machine is an intricate and highly organized process.
73 Analysis of PSII knock-out mutants of the cyanobacterium *Synechocystis* sp. PCC 6803
74 (hereafter *Synechocystis*) has revealed that the large pigment-binding proteins first associate with
75 their neighboring LMM subunits to form small building blocks (or modules) which then
76 sequentially assemble via a series of intermediates to form the functional PSII complex
77 (Komenda et al., 2012b) .

78 In the earliest stage of PSII biogenesis, the D1 and D2 subunits form modules (D1_{mod}, D2_{mod})
79 with adjacent small PSII proteins and auxiliary factors. D1_{mod} was shown to contain PsbI, Ycf48,
80 Ycf39 and HliC/D (Dobáková et al., 2007; Knoppová et al., 2014) while D2_{mod} contains both the
81 PsbE and PsbF subunits of Cyt *b*₅₅₉ (Komenda et al., 2008) and CyanoP (Knoppová et al., 2016).
82 So far, no information about their pigment content has been reported. D1_{mod} and D2_{mod} then
83 combine to form the PSII reaction center assembly complex, RCII (Komenda et al., 2008;
84 Knoppová et al., 2014; Kiss et al., 2019). The subsequent attachment of CP47_{mod} results in the
85 formation of the RC47 intermediate (Boehm et al., 2011; Boehm et al., 2012) which then binds
86 CP43_{mod} (Boehm et al., 2011) to give rise to the monomeric PSII core complex, RCCII. The final

87 steps involve the light-driven formation of the Mn_4CaO_5 cluster, the attachment of the luminal
88 subunits, and dimerization of the PSII complex. The process of PSII biogenesis is assisted by
89 several step-specific auxiliary or assembly factors, many of unclear function (Nixon et al., 2010;
90 Komenda et al., 2012b; Heinz et al., 2016). PSII biogenesis in chloroplasts follows a similar
91 sequence of events (Nickelsen and Rengstl, 2013) and is assisted by homologous as well as
92 chloroplast-specific auxiliary factors (Lu, 2016).

93 The transient nature and low accumulation of assembly complexes have hindered their detailed
94 analysis. Nevertheless, a combination of protein tagging (either His-tag or FLAG-tag) and the use
95 of appropriate mutants that block assembly at a specific step has allowed the isolation and
96 characterization of the CP43 and CP47 modules (Boehm et al., 2011; Bučinská et al., 2018) and
97 the RC47 complex (Boehm et al., 2012).

98 Using a FLAG-tagged derivative of the Ycf39 assembly factor, we have also isolated and
99 characterized the protein composition and spectral characteristics of one type of RCII complex
100 (called RCII*) associated with Ycf39 and High-light inducible proteins (Hlips) (Knoppová et al.,
101 2014). The Ycf39 and single-helix Chl- and β -carotene (β -car) binding Hlips (Komenda and
102 Sobotka, 2016) form a stable sub-complex that is implicated in the photoprotection of RCII
103 (Komenda et al., 2008; Knoppová et al., 2014).

104 Isolated thylakoid membranes also contain a smaller RCII complex called RCIIa (Komenda et al.,
105 2008; Knoppová et al., 2014) which does not bind the Ycf39/Hlips complex. The Ycf39/Hlips
106 complex can be detached from the isolated RCII* *in vitro* (Knoppová et al., 2014) but the
107 relationship between RCIIa and RCII* during the biogenesis of PSII *in vivo* is not yet clear.

108 We show here that isolated RCII complexes perform light-driven primary charge separation and
109 have a pigment composition that corresponds well to that found in the D1/D2 part of the PSII
110 crystal structure (Umena et al., 2011). Several newly identified proteins that co-purify with RCII
111 might play a role in PSII biogenesis. Moreover, our data suggest that RCII* and RCIIa are
112 formed independently via distinct assembly pathways. We also isolated and characterized
113 FLAG-tagged D1_{mod} and D2_{mod}. Both modules lacked pheophytin *a* (Pheo) but contained
114 neighboring small PSII subunits and several co-purifying proteins that might represent previously
115 unidentified D1- and D2-specific assembly factors. Stably bound Chl was detected just in D1_{mod}.

116

117 **RESULTS**

118 **Spectral properties and protein composition of RCII complexes isolated using a His-tagged**
119 **D2 subunit**

120 We have shown previously that RCII complexes accumulate to low but detectable levels when
121 PSII assembly is blocked due to the lack of the PSII inner antenna CP47 (Komenda et al., 2004;
122 Knoppová et al., 2014). To isolate RCII complexes, we first introduced a modified *psbDI* gene
123 coding for D2 with an N-terminal 6xHis tag into the previously characterized Tol145 strain
124 depleted in phycobilisomes and lacking both *psbD* genes (Tang et al., 1993). In a second step, we
125 inactivated the *psbB* gene coding for the CP47 antenna to produce the His-D2/ Δ CP47 strain.
126 Two-dimensional gel electrophoresis consisting of clear native (CN) electrophoresis in the first
127 dimension followed by SDS-PAGE in the second dimension confirmed that His-D2/ Δ CP47
128 accumulated small amounts of RCII complexes, denoted RCII* and RCIIa, similar to the Δ CP47
129 strains characterized previously (Komenda et al., 2008; Knoppová et al., 2014). The slightly
130 lower mobility of the D2 protein identified in the second dimension suggested successful
131 incorporation of His-tagged D2 into RCII complexes (Fig. S1).

132 To purify RCII complexes, membranes isolated from the His-D2/ Δ CP47 strain were solubilized
133 using the mild detergent β -dodecyl-D-maltoside (DM) and subjected to nickel (Ni) affinity
134 chromatography. After extensive washing the final eluate showed a similar absorption spectrum
135 to that of plant or *Synechocystis* PSII reaction center complexes (PSII RC) prepared by detergent
136 extraction of the CP47 and CP43 antennae from larger PSII core complexes (Fig. 1; compare
137 with Fig. 2 in Oren-Shamir et al. (1995) and Tomo et al. (2008)). However, the Chl red
138 absorption maximum of our preparation was blue-shifted by about 3 nm indicating the prevalence
139 of more blue-absorbing Chl forms (with maxima at 670-671 nm) over the forms absorbing at
140 longer wavelengths. The low temperature Chl fluorescence spectrum had a main maximum at
141 682 nm which is also similar to that identified by Tomo et al. (2008). A small fluorescence
142 shoulder at 720 nm indicated the possible presence of PSI (see below).

143 To characterize the complexes present in the preparation, we used two-dimensional gel
144 electrophoresis. As shown in Fig. 1C the preparation was heterogeneous and contained several
145 types of complex in line with previously published data (Komenda et al., 2008; Knoppová et al.,
146 2014). We detected the presence of the two complexes previously designated RCII* and RCIIa
147 with masses of about 200 and 150 kDa, respectively. A combination of immunoblotting and mass

148 spectrometry confirmed that both RCII* and RCIIa contain the D1, D2, PsbE, PsbF and PsbI
149 subunits of PSII, as well as the assembly factors Ycf48 (Komenda et al., 2008; Yu et al., 2018)
150 and the more recently described RubA (Kiss et al., 2019). As already noted, RCII* differs from
151 RCIIa by association with the Ycf39/Hlips complex (Knoppová et al. 2014), which was also
152 confirmed in our new preparation (Fig. 1C).

153 Torabi et al. (2014) have suggested the involvement of PsbN in the formation of the RCII
154 complex in tobacco (*Nicotiana tabacum*). Using specific antibodies raised against *Synechocystis*
155 PsbN, we detected PsbN in both RCII* and RCIIa (Fig. 1C) with PsbN more abundant in RCII*
156 than in RCIIa. Moreover, the preparation also contained another putative PSII-related protein,
157 Slr0575, a homologue of the plant Acclimation of Photosynthesis to the Environment 1 protein,
158 APE1 (Walters et al., 2003). After separation by CN-PAGE the Slr0575 protein was mostly
159 found in the unassembled protein fraction, but some remained associated with RCII*. The
160 presence of Slr0575 in RCII* was confirmed by re-analysis of the previously characterized
161 FLAG-Ycf39 preparation (Fig. S2).

162 We also constructed a His-D2/ Δ CP47 mutant that lacked Ycf39. As anticipated, the isolation of
163 RCII from this strain confirmed the loss of the RCII* complex and the accumulation of the RCIIa
164 complex (Fig. S3). RCIIa was separated into two closely spaced fluorescent bands with the larger
165 one containing an additional protein identified as Slr1470 by mass spectrometry (MS, Table S1).

166 The amounts of RCII* and RCIIa detected in cells of CP47-less strains are usually very similar
167 (see Fig. S1). To test whether there is a precursor-product relationship between them, with one
168 converting into the other, we performed a classic radioactive pulse-chase experiment using cells
169 of the CP47-less strain. Both D1 and D2 were labeled in both complexes to a similar extent
170 during the pulse and the label in both proteins declined similarly in RCII* and RCIIa, indicating
171 no clear inter-conversion between these two complexes (Fig. S4). Thus, we propose that each
172 complex is formed independently via a distinct assembly pathway.

173

174 **Identification of a RCIIa/PSI assembly complex**

175 In addition to the RCII* and RCIIa complexes, the His-D2 preparations also contained larger
176 Chl-containing complexes: a fluorescent one of mass about 350 kDa containing the same protein
177 components as RCIIa and most probably representing its dimer, and a larger, much less

178 fluorescent one, of about 450 kDa. The latter complex also contained components of RCIIa, but,
179 in addition, showed the presence of PSI subunits. Based on its size, the complex likely represents
180 RCIIa bound to a PSI monomer (RCIIa/PSI; Fig. 1C). The content of RCIIa/PSI in the
181 preparations was highly variable as documented by its higher level in another preparation isolated
182 under the same conditions (Fig. S5). To verify the composition of the complexes and judge
183 whether the formation of the RCIIa/PSI complex was an isolation artifact of the Ni affinity
184 purification procedure, we compared the His-D2 preparation with another preparation isolated
185 using FLAG affinity chromatography from a CP47-less strain expressing a C-terminally FLAG-
186 tagged PsbI subunit (PsbI-FLAG). Both preparations consisted of similar complexes including
187 RCIIa/PSI (Fig. 1 and Fig. S6). In addition, the FLAG-based purification provided a preparation
188 devoid of most of the non-specific components identified in the His-D2 preparation (compare the
189 control His- and FLAG-tag pull-downs in Fig. S7 and Fig. S8, respectively).

190 Prohibitin 3 (Phb3, Slr1128; Boehm et al., 2009) and FtsH2/FtsH3 complexes were present in
191 both the His-D2 and the control WT pull-down together with elongation factor EF-Tu, a typical
192 contaminant of our His-tag preparations (Fig. S1 and S7). The PsbI-FLAG preparation (Fig. S6)
193 also contained both Phb3 and FtsH2/FtsH3, and additionally prohibitin 1 (Phb1, Slr1106), but all
194 these proteins were absent in the control FLAG-tag pull-down (Fig. S8). We therefore conclude
195 that FtsH2/FtsH3, Phb1 and Phb3 are authentic components of RCII preparations. These
196 components were also identified by MS analysis (Table S2).

197

198 **Primary charge separation in RCII complexes**

199 The D1-D2 heterodimer binds the Chl and Pheo molecules involved in the light-induced primary
200 charge separation step within PSII. The primary electron donor, P680, is considered to be a
201 collection of four special Chl molecules bound to D1 and D2 whereas the primary electron
202 acceptor Pheo is bound specifically to D1 (Diner and Rappaport, 2002; Romero et al., 2012).
203 Light-induced electron transfer from P680 to Pheo results in the formation of the $P680^+Pheo^-$
204 radical pair (Diner and Rappaport, 2002). Primary charge separation also occurs in plant and
205 cyanobacterial PSII RC complexes prepared by detergent-induced removal of the CP43 and CP47
206 antenna complexes from larger PSII core complexes (Nanba and Satoh, 1987; Giorgi et al., 1996;
207 Tomo et al., 2008).

208 To judge whether the RCII assembly complexes isolated here were capable of primary charge
209 separation, we measured the reversible light-induced absorption difference spectra in the range
210 650-710 nm. This measurement was performed either in the presence of the electron acceptor,
211 SiMo, to detect the accumulation of the oxidized primary donor, P680⁺, or in the presence of
212 sodium dithionite to detect reduction of the primary electron acceptor Pheo, according to Vácha
213 et al. (2002). Both methods (Fig. 2) gave similar results to those obtained with the isolated plant
214 PSII RC complex (Vácha et al., 2002). These data showed that at least some of the RCII
215 assembly complexes can perform the primary photochemical reaction and therefore should
216 contain the complete set of pigments required for these reactions. Because our RCII preparations
217 contained variable amounts of the monomeric PSI complex associated with many more Chl
218 molecules (Malavath et al., 2018) than the RCII complexes, precise quantification of the
219 photoactive P680 or Pheo was not reliable. Instead, we focused on further purification of each
220 RCII complex from the crude His-D2 preparation to assess their individual spectral properties
221 and pigment composition.

222

223 **Pigment composition of individual RCII complexes**

224 To separate RCII* and RCIIa we used semi-preparative CN-PAGE as the similar size of RCII
225 complexes did not allow their separation using gel filtration, and ionex chromatography was also
226 unsuccessful (Fig. S9). Separated complexes from several CN gel lanes were eluted from the gel
227 and characterized using absorption and 77 K fluorescence spectroscopies and pigment
228 composition was determined using HPLC. The overlay of absorption spectra of the RCII* and
229 RCIIa complexes normalized to the 415 nm absorption maximum showed that they have the
230 same position of the red maximum of Chl at 672 nm and mainly differed in the content of
231 carotenoids absorbing in the 430-520 nm region (Fig. 3A). The 77 K Chl fluorescence spectra
232 were practically identical with a maximum at 685 nm, which is similar to the fluorescence
233 maximum displayed by PSII RCs isolated by fragmentation (Tomo et al., 2008). The RCIIa
234 complex did show a slightly higher satellite peak at 740 nm than RCII* (Fig. 3B).

235 We also measured both types of spectra for the RCIIa/PSI complex containing the PSI monomer
236 and RCIIa complex. The red absorption peak was red-shifted by 4 nm due to the red-absorbing
237 Chls of the PSI monomer (Fig. 3A). Interestingly, the 77 K Chl fluorescence spectrum showed a

238 typical peak of RCII at 680 nm and that of PSI at 720 nm but there was also a shoulder around
239 675 nm (Fig. 3B), which is typical for Chl molecules in detergent or lipid micelles (Trinugroho et
240 al., 2020). No such 675-nm shoulder was observed in RCII* or in RCIIa.

241 We subsequently performed a detailed HPLC analysis of Chls, carotenoids and heme-*b* (Fig. 4A).
242 Heme-*b* was used as a standard for normalization of the pigment content as exactly one heme-*b*
243 (Cyt *b*₅₅₉) should be present in all types of RCII complexes (Table 1). The pigment composition
244 of RCIIa was similar to that previously determined for the *Synechocystis* PSII RC complex
245 prepared by stripping the CP47 and CP43 inner antennae from the complete PSII core complex
246 (Tomo et al., 2008). Based on the crystal (Umena et al., 2011) and cryo-EM (Gisriel et al., 2020)
247 structures of PSII, the 6 Chl are likely to represent the four central Chls belonging to the P680
248 oligomer plus Chl_{Z_{D1}} and Chl_{Z_{D2}} ligated by D1-His118 and D2-His117 on the periphery of the
249 RCII complex, respectively. Our measurements also support the presence of 1-2 predicted
250 carotenoids in the D1/D2 heterodimer. RCII* contained an additional three Chl and a single β-car
251 molecule which can be attributed to the presence of the Ycf39/Hlip complex. We also analyzed
252 the RCIIa/PSI complex and given the expected 1:1 ratio between PSI and RCII based on the
253 estimated size of the complex, it is interesting that the PSI complex appears to contain on average
254 only about 60 Chls, which is much less than the value of 95 Chls predicted from the known
255 structure of monomeric PSI (Malavath et al., 2018).

256

257 **Isolation of D1 and D2 assembly modules**

258 To investigate the steps preceding RCII assembly, we isolated and characterized unassembled
259 forms of both D1 and D2. Both these forms are associated with adjacent small PSII subunits and
260 several auxiliary factors and are termed D1 and D2 modules (D1_{mod} and D2_{mod}). For their
261 isolation, we constructed new strains expressing N-terminal FLAG-tagged versions of D1 and D2
262 (FLAG-D1/ΔPSII and FLAG-D2/ΔPSII, respectively) in the previously constructed ΔPSII strain
263 lacking the *psbA*, *psbB*, *psbC* and *psbD* genes encoding D1, CP47, CP43 and D2, respectively
264 (Trinugroho et al., 2020). The corresponding FLAG-tagged D1 and D2 assembly modules were
265 then isolated using immunoaffinity chromatography.

266 The Chl and carotenoid content of the isolated FLAG-D1 preparation was low and consequently
267 the absorption spectra of the preparation (Fig. 5A) displayed an unusually large maximum around

268 620 nm indicating an increased level of contaminating phycocyanin which has been previously
269 detected in FLAG-specific pulldowns (Knoppová et al., 2014). Its relatively high content is most
270 probably related to the very low cellular level of unassembled D1 and the need for extensive
271 concentration of the preparation, so that even small amounts of contaminating protein become
272 strongly pronounced. The red peak of Chl absorption with a maximum of about 677 nm (Fig. 5A)
273 suggested the presence of PSI and this was confirmed from the 77 K Chl fluorescence spectrum
274 (Fig. 5B) which exhibited a lower maximum at 720 nm belonging to PSI-bound Chl. There was
275 also a peak at 675 nm indicating weakly associated Chl bound in lipid/detergent envelope of the
276 protein. On the other hand, the fluorescence maximum at 683 nm showed the presence of Chl
277 specifically associated with FLAG-D1 since it was missing in the control preparation from the
278 FLAG-free Δ PSII strain lacking all four large PSII Chl-proteins (Fig. S10B). The stable binding
279 of Chl to the FLAG-D1 was also confirmed by the detection of Chl fluorescence (Fig. 6, 1D fluor
280 and 2D Chl, red arrows) at the position of the main FLAG-D1 band (Fig. 6, 2D SYPRO stain and
281 2D blots, blue arrows) on the 1D and 2D gels. HPLC analysis of the preparation (Fig. 4B)
282 confirmed the presence of Chl and β -car, which might, however, partly belong to contaminating
283 PSI. Most importantly, no Pheo or heme was detected in the preparation.

284 A 2D immunoblot analysis confirmed the isolation of the FLAG-tagged D1 protein together with
285 PsbI, Ycf39 and Ycf48. Based on its staining intensity, Ycf48 looked to be present at a ratio of
286 close to 1:1 with the main D1 protein band (Fig. 6, F.D1 with a blue arrow). Additional protein
287 bands were also present in the preparation. Apart from the PSI trimer and monomer there was
288 also a large abundance of ribosomal subunits, which are all likely contaminants present in this
289 highly concentrated preparation of a rare FLAG-tagged protein. This is confirmed by the high
290 abundance of ribosomal subunits in the control preparation lacking a FLAG tag (Fig. S8, right
291 panel). Immunoblotting also revealed the presence of the prohibitin homologue Phb3 and the
292 FLAG-D1 specific co-elution of this protein together with the previously mentioned components
293 Ycf39 and Ycf48 was confirmed by MS analysis (Tables 2 and S3).

294 The absorption spectrum of the isolated FLAG-D2 preparation was characterized by a small peak
295 at 559 nm and a sharp main maximum at 429 nm suggesting the presence of Cyt b_{559} (Figs. 5A
296 and S10A). The 77 K Chl fluorescence emission spectrum had a small peak at 721 nm again
297 suggesting the presence of PSI while the dominating band peaked at 675 nm indicating the
298 presence of Chl weakly bound in the lipid/detergent envelope of the protein (Figs. 5B and S10B).

299 This was confirmed by the absence of a distinct Chl fluorescence band in the 1D CN gel (Fig. 6,
300 1D fluor, red arrow) at the position of the main FLAG-D2 band (Fig. 6, 2D SYPRO stain and
301 FLAG blot, blue arrows). Instead, we detected a smeared 2D Chl fluorescence underneath the
302 broadened part of the Flag-D2 band (Fig. 6, 2D Chl, red rectangles). Protein analysis confirmed
303 the presence of contaminating PSI complexes, phycocyanin and ribosomal subunits while the
304 stained components were identified as FLAG-D2 and the PsbE and PsbF subunits of Cyt *b*₅₅₉
305 (Fig.6). The other specific components detected in the preparation by immunoblotting were
306 CyanoP, FtsH3 and the two prohibitin homologues Phb1 and Phb3. The small amount of Ycf48
307 can be considered unspecific, since similar trace amounts of the protein were found in the control
308 (Fig. S8). MS analysis (Tables 2 and S4) confirmed the components detected by the
309 immunoblotting and identified several other specific proteins including FtsH2, Slr1470 and PsbY,
310 which is a PSII subunit localized in some structural models of PSII in the vicinity of PsbE
311 (Guskov et al., 2009; Kato et al., 2021). Besides the presence of Chl and β -car, which are likely
312 to be due to PSI contamination, we detected a high content of heme belonging to Cyt *b*₅₅₉ but no
313 Pheo (Fig. 4B). Interestingly, the absorption peak at 559 nm suggested that Cyt *b*₅₅₉ was present
314 in its reduced form which is unusual for isolated PSII complexes (Shinopoulos and Brudvig,
315 2012).

316

317 **Discussion**

318 **RCII* and RCIIa are distinct assembly complexes**

319 RCII assembly complexes are normally undetectable in WT and have only been observed in cells
320 grown at low temperature (Komenda et al., 2008). Increased levels are, however, observed in
321 either mutants lacking the CP47 subunit (Komenda et al., 2004) or mutants impaired in the de
322 novo biosynthesis of Chl needed for efficient CP47 accumulation (Hollingshead et al., 2016).
323 Although the level of RCII complexes in CP47 knock-out strains is less than 10 % of PSII in WT
324 cells (Komenda et al., 2004), this was sufficient for isolation and characterization.

325 We show here that the main RCII complexes present in preparations isolated using either His-
326 tagged D2 (Fig. 1) or FLAG-tagged PsbI (Fig. S6) in a CP47 deletion background are the
327 previously identified RCII* and RCIIa complexes (Komenda et al., 2008). Both complexes
328 contain D1, D2, the PsbE and PsbF subunits of Cyt *b*₅₅₉, PsbI and the lumenally exposed Ycf48

329 accessory factor but only RCII* contains the Ycf39/Hlip complex (see Knoppová et al., 2014).
330 Ycf39 belongs to the family of short-chain dehydrogenase/reductases but it remains unclear
331 whether Ycf39 has a catalytic activity or has evolved an alternative function such as binding
332 mRNA (for review see Kavanagh et al. (2008)). Ycf39 binds to a pair of Hlips ligating 4-6 Chls
333 and 2 β -cars, which can quench Chl excited states via energy transfer to an S₁ state of β -car
334 (Staleva et al., 2015) thereby potentially protecting RCII* from photodamage (Knoppová et al.,
335 2014).

336

337 **Proteins that co-purify with RCII and the D1 and D2 modules**

338 The only accessory protein factors present in close to stoichiometric amounts with respect to the
339 main RCII components were Ycf48 in both complexes, Ycf39/Hlips in RCII* and RubA in
340 RCIIa. We could not detect RubA in either D1_{mod} or D2_{mod} although we have previously co-
341 isolated RubA and D1 with FLAG-Ycf39 from the D2-less strain (Knoppová et al., 2014; Kiss et
342 al., 2019). RubA is thought to facilitate the mutual binding of D1_{mod} and D2_{mod} so its greater
343 abundance in RCII might reflect tighter binding due to interactions with both modules.

344 In addition, we have now identified several additional factors that are present at sub-
345 stoichiometric levels and thus not easily observed in stained gels, but which are clearly detectable
346 by immunoblotting and MS analyses. The presence of these factors causes microheterogeneity
347 within the population of RCII complexes which is manifested in 1D native gels as double bands
348 (Fig. S3) and on 2D gels by broader bands of the major components that extend horizontally
349 towards higher molecular mass (for instance bands of D1 and D2 in RCII* in Figs. 1, S2, S5 and
350 S6).

351 One of these factors is the PsbN protein, which has previously been detected in tobacco
352 (*Nicotiana tabacum*) RC assembly complexes but not in any type of cyanobacterial PSII. The
353 *Synechocystis* PsbN protein does not contain positively charged amino acids and is therefore less
354 easy to detect by an ordinary MS bottom-up analysis after trypsin cleavage. Its higher level in
355 RCII* appears to be complementary to lower levels of RubA in the same sub-complex (Fig. S6),
356 possibly suggesting neighboring or overlapping binding sites for both components. The previous
357 deletion of the *psbN* gene in *Synechocystis* (Mayes et al., 1993) did not exhibit any apparent
358 effect on the photoautotrophic growth of the mutant. However, PsbN in tobacco is required for

359 repair from photoinhibition and efficient assembly of RCII (Torabi et al., 2014), which is in
360 agreement with our localization of the protein within this complex. Similarly, RubA is also
361 needed for PSII repair and RCII formation in *Synechocystis* (Kiss et al., 2019) and
362 *Chlamydomonas* (García-Cerdán et al., 2019).

363 Another component found in RCII is the Slr0575 protein which together with CyanoP appears to
364 bind mostly to RCII* (Fig. S2). The *Arabidopsis* (*Arabidopsis thaliana*) homologue of Slr0575 is
365 APE1 (corresponding gene is *At5g38660*), which has been detected in the *Arabidopsis* complex
366 equivalent to RCII*, consisting of One Helix Protein 1 (OHP1) and One Helix Protein 2 (OHP2)
367 (plant homologues of Hlips), D1, D2, High Chlorophyll Fluorescence 136 (HCF136, plant
368 homologue of Ycf48) and High Chlorophyll Fluorescence 244 (HCF244, plant homologue of
369 Ycf39) (Myouga et al., 2018). Our identification of Slr0575 in RCII* (Figs. 1 and S2) provides
370 important support for a conserved role for Slr0575/APE1 in the early steps of PSII biogenesis.
371 Such a role is consistent with the phenotype of the *ape1* mutant of *Arabidopsis* which is defective
372 in increasing the levels of PSII upon a transition from low to high light (Walters et al., 2003). In
373 contrast, the *Synechocystis* deletion mutant did not show any substantial phenotypic changes
374 when compared with WT (Thompson, 2016).. However, when we deleted this gene in the Δ CP47
375 strain and compared protein synthesis in Δ CP47 and the Δ CP47/ Δ Slr0575 double mutant, the
376 latter showed a 50 % higher labelling of D2 within the RCIIa complex compared to CP43 and
377 PSI large subunits PsaA/B (Fig. S11). Since protein staining of the 2D gel did not show any
378 apparent increase in the accumulation of RCII in the double mutant, the result indicates that
379 Slr0575 increases the stability of unassembled D2. In agreement with this, we found traces of
380 Slr0575 in the Flag-D2 but not in the FLAG-D1 preparation.

381 The Slr1470 subunit was detected as a Coomassie Blue stained band in the RCIIa complex
382 isolated from the Ycf39-less strain (Fig. S3) and was also detected in the Flag-D2 preparation but
383 not in the FLAG-D1 or PsbI-FLAG preparations. Slr1470 is predicted in Uniprot to possess a
384 single transmembrane helix and a bacterial pleckstrin homology domain (InterPro entry
385 IPR012544) which is implicated in lipid binding (Xu et al., 2010). The gene for Slr1470 is
386 conserved among oxygenic phototrophs (the homologous gene in *Arabidopsis* is *ATIG14345*)
387 and our attempts to delete the gene were not successful indicating its crucial importance.

388 We also found that prohibitin subunits, Phb1 and Phb3, and FtsH2/FtsH3 protease complexes co-
389 purified with PsbI-FLAG tagged RCII preparations (Fig. S6) but were absent from control non-
390 FLAG preparations (Fig. S8). The presence of the FtsH2/FtsH3 complex might be related to the
391 targeting of RCII for degradation (Krynická et al., 2015). Prohibitins are structurally related to
392 HflC/K proteins that form large supercomplexes with FtsH protease complexes in *Escherichia*
393 *coli* and regulate FtsH activity (Saikawa et al., 2004). Indeed, the *Synechocystis* prohibitin
394 homologue, Phb1, has previously been detected in affinity-purified FtsH2/FtsH3 preparations but
395 at a much lower level than that found here in the RCII preparations (Boehm et al., 2012). MS
396 analysis of the PsbI-FLAG preparation (Table S2) also revealed the specific presence of another
397 FtsH protease FtsH4 of unknown function, the thylakoid curvature homologue CurT (Slr0483)
398 and CP43. Possibly these proteins are located in the vicinity of RCII complexes when CP47 is
399 absent.

400 It is perhaps not surprising that the FtsH2/FtsH3 protease complex together with Phb1 were
401 detected in D2_{mod}, since we have previously shown that the level of unassembled D2 is controlled
402 by FtsH2/FtsH3 (Komenda et al., 2006). Therefore, D2_{mod} is expected to be targeted by this
403 protease complex for degradation. The absence of FtsH2/FtsH3 and Phb1 in D1_{mod} is also in
404 agreement with our previous data demonstrating a negligible effect of the FtsH2 deletion on the
405 level of unassembled D1 (Komenda et al., 2010). Together these data suggest that either the site
406 of D1_{mod} formation in cells differs from that of D2_{mod} as suggested by Schottkowski et al. (2009),
407 or that D1_{mod} is not recognized by FtsH2/FtsH3, for instance due to the binding of Ycf48.

408 More surprising is the association of D1_{mod}, D2_{mod} and RCII with the Phb3 protein which has
409 been previously detected in the plasma membrane fraction obtained using a two-phase
410 partitioning technique (Boehm et al., 2009). Possibly Phb3 is located at the junction of the
411 thylakoid and plasma membranes in a region called the thylapse where PSII biogenesis might be
412 initiated (Rast et al., 2019). Phb3, which forms a large circular homocomplex, is more closely
413 related to stomatins than the prohibitins (Boehm et al., 2009). The role of stomatins remains
414 unclear but they have been implicated in regulating the structural organization of membranes
415 which would be consistent with a location for Phb3 in the thylapse (Rast et al., 2019).

416 Although our previous characterization of Phb1 and Phb3 in *Synechocystis* did not reveal a
417 crucial role for these proteins in PSII repair/biogenesis (Boehm et al., 2009), their association

418 with $D1_{\text{mod}}$, $D2_{\text{mod}}$ and RCII suggested a possible involvement in the stability of these PSII
419 assembly intermediates. To test the stabilizing role of Phb3, we deleted the *phb3* gene in the
420 ΔCP47 and ΔCYT strains lacking CP47 and Cyt b_{559} , respectively. In both cases the deletion did
421 not affect the levels of $D1_{\text{mod}}$, $D2_{\text{mod}}$ and RCII leaving the importance of Phb3 unclear.

422 As expected from previous analyses, the $D1_{\text{mod}}$ contains PsbI, which binds to the first and second
423 transmembrane helices of D1, plus Ycf48 which docks on to the luminal surface of D1
424 (Komenda et al., 2008, Yu et al., 2018). $D2_{\text{mod}}$ contains Cyt b_{559} subunits at stoichiometric levels
425 (Komenda et al., 2008), and present at lower levels are PsbY, which binds to PsbE (Guskov et al.,
426 2009), and Cyanop, a lipoprotein that binds to luminal surface of D2 (Cormann et al., 2014;
427 Knoppová et al., 2016) (Table 2).

428

429 **The complex of RCIIa with monomeric PSI and its physiological relevance**

430 Unlike RCII*, RCIIa was also detected in a binary complex with a PSI monomer (Fig. 1C, see
431 below) which added another layer of complexity to the RCII preparations. The RCIIa/PSI
432 complex was present in both the His-D2 and PsbI-FLAG preparations indicating that it is not an
433 artifact related to the unspecific binding of PSI to the isolation resin. When membranes of the
434 His-D2/ ΔCP47 strain were solubilized with different concentrations of DM before His-D2
435 purification, the RCIIa/PSI complex was obtained preferentially at lower DM concentrations
436 while an increased amount of DM led to its decreased level while the content of both RCII
437 complexes in the preparation increased (Fig. S12). Surprisingly, we were unable to detect
438 RCIIa/PSI in solubilized membranes isolated from the CP47-less strain (see Fig. S1). Our
439 interpretation of these results is that RCIIa/PSI is unstable and can be stabilized by binding to the
440 isolation resins while at higher detergent concentration it becomes disrupted again. The marked
441 increase in yield of RCII* and RCIIa obtained by extracting at higher detergent levels suggests
442 that these complexes reside in membrane regions that are not as easily solubilized as standard
443 thylakoids which are normally solubilized completely at both 1.5 and 3 % (w/v) DM. These
444 regions might be related to so-called lipid rafts or detergent-resistant membranes (DRMs) which
445 were originally described in eukaryotic cells but are now recognised to be present in bacterial
446 membranes (for review see Lopez and Koch (2017)). A hallmark of DRMs is the presence of
447 members of the band 7 protein or SPFH family (consisting of the stomatin, prohibitin, flotillin,

448 and HflK/C proteins) (Rivera-Milla et al., 2006) and so it is notable that we could detect Phb1
449 and Phb3 in RCII preparations. Overall, our data support the concept that thylapses, the proposed
450 site of PSII biogenesis (Rast et al., 2019), could represent a specialised detergent-resistant
451 membrane.

452

453 **Pigment composition of RCII complexes and D1/D2 assembly modules**

454 The electrophoretically purified RCIIa complex showed absorption and low temperature
455 fluorescence spectra that were in line with those previously reported for PSII RCs isolated after
456 stripping CP43 and CP47 from plant PSII-enriched membrane particles (Nanba and Satoh, 1987;
457 Gounaris et al., 1990) or from *Synechocystis* PSII complexes using high concentrations of Triton
458 X-100 (Gounaris et al., 1989; Oren-Shamir et al., 1995; Tomo et al., 2008). The main difference
459 was a blue-shifted maximum of the Chl red absorption peak (from 676 nm in plant to 672 nm in
460 our *Synechocystis* complex; Fig. 3). The observed ratio of two Pheos, 1-2 carotenoids and six
461 Chls per Cyt *b*₅₅₉ suggests the binding of a full complement of pigments to the D1/D2
462 heterodimer in RCII. The low amounts of complex precluded the detection of plastoquinone by
463 HPLC so the presence of bound quinone cannot be excluded. The RCII* complex had a higher
464 content of Chl and β -car than RCIIa due to the presence of pigment-containing Ycf39/Hlips
465 complex (Table 1; Knoppová et al., 2014; Staleva et al., 2015). However, the isolated Ycf39-Hlip
466 complex alone binds 4 - 6 Chls and two β -cars (Staleva et al., 2015; Shukla et al., 2018), thus
467 RCII* appears to have two or three Chls less than expected. One possible explanation is that
468 Ycf39/Hlip has delivered some of its Chl to RCII. The presence of a sufficient set of pigments
469 (Chls, pheophytins) needed for charge separation in both RCII* and RCIIa suggests that both
470 complexes possess this basic photochemical activity. We did not directly measure the individual
471 activities of RCII* and RCIIa due to their low yields; this measurement was feasible only for the
472 crude His-D2 preparation containing both types of RCII complex (Fig. 2).

473 The analysis of D1_{mod} and D2_{mod} by CN gel electrophoresis and subsequent detection of Chl
474 fluorescence indicated that the main band of D1_{mod} is fluorescent and therefore stably binds Chl.
475 In contrast, the D2 main band was not fluorescent and its broadened part showed just a weak
476 fluorescence with a low temperature emission maximum at 675 nm (Fig. 5 and Fig. S10)
477 corresponding to detergent/lipid-associated Chl or Chl bound to non-native binding sites in D2.

478 Thus, D2_{mod} appears Chl-deficient or possibly has weakly bound Chl that is easily lost during
479 isolation and/or analysis. This difference between D1_{mod} and D2_{mod} might be related to the
480 binding of Ycf48 to the luminal side of D1 and Ycf39 to the cytoplasmic side, thereby helping to
481 stabilize the tertiary structure of D1 and binding of Chl (Knoppová et al., 2014; Yu et al., 2018).
482 PsbI, which binds to the first and second transmembrane helices of D1 may also stabilize binding
483 of Chl ligated by His118 of D1 (Dobáková et al., 2007; Umena et al., 2011). Importantly, we
484 were unable to identify Pheo in either D1_{mod} or D2_{mod} suggesting that this pigment is inserted or
485 formed within RCII or during the association of D1_{mod} and D2_{mod}.

486

487 **Two possible pathways for the assembly of RCII complexes**

488 The existence of two main, seemingly independent populations of RCII complexes with specific
489 protein components indicates that cyanobacteria might possess different pathways of RCII
490 biogenesis. We have considered the possibility that the Ycf39/Hlips-containing RCII* with an
491 incomplete complement of Chl (Table 1) could have its origin in a de novo process, while RCIIa
492 could be formed in a repair-like process, in which pigments released from degraded D1 and D2
493 subunits would be immediately reintroduced into newly synthesized proteins, resulting in RCII
494 with a complete set of pigments. To test this idea, we analyzed the RCII preparation from a His-
495 D2/ Δ CP47 strain additionally lacking the FtsH2 (Slr0228) subunit of the FtsH2/FtsH3 protease
496 complex and so impaired in the degradation of damaged PSII (Komenda et al., 2006). This
497 mutant accumulated similar amounts of both RCII* and RCIIa as in the original His-D2 strain
498 and the complexes also had the same pigment composition as the corresponding complexes of the
499 original strain (Fig. S13). The only apparent difference was the almost exclusive presence of the
500 mature D1 protein in the FtsH2-lacking strain. This can be explained by an increase in the time
501 available for D1 maturation due to inhibited turnover of D1 and D2 (Komenda et al., 2006).
502 Thus, it is unlikely that RCIIa comes from the repair process.

503 The above results led us to the idea of two distinct pathways for the assembly of RCII complexes.
504 One would lead to RCIIa via a combination of D1_{mod} and D2_{mod} without participation of the
505 Ycf39/Hlips complex. Instead, PSI monomeric complexes located in the vicinity would provide
506 photoprotection via energy spill-over and help deliver Chl to RCIIa to give rise to a Chl-depleted
507 sub-population of PSI (Kopečná et al., 2012). Indeed, the gel-purified RCIIa-associated PSI(1)

508 complex was depleted by about 15 Chls in comparison to PS(1) complexes purified from the
 509 CP47-less strain. In agreement with this model, quantification of RCII complexes in membranes
 510 of a strain lacking PSI, CP43 and CP47 showed an approximate four-fold higher abundance of
 511 RCII* over RCIIa, with the latter possibly formed from release of the Ycf39/Hlip complex from
 512 RCII* during the analysis by CN PAGE (Fig. S14). A similar prevalence of RCII* over RCIIa
 513 has been observed in the PSI-deficient strains generated by deleting PsbH and both PsbH and
 514 Pam68 (Bučinská et al., 2018).

515 The second pathway requires the assistance of the Ycf39/Hlips complex both to provide
 516 photoprotection and deliver Chl to RCII. We hypothesize that this route is the only pathway for
 517 building PSII in chloroplasts as the Ycf39 homologue, HCF244, together with the Hlip
 518 homologues OHPs are strictly required for D1 synthesis, RCII formation and PSII accumulation
 519 (Link et al., 2012; Hey and Grimm, 2018) while in *Synechocystis* RCIIa is formed in the absence
 520 of Ycf39. Additional support for this hypothesis comes from the experiments of Muller and
 521 Eichacker (1999) who detected a D2 assembly complex in etioplasts that lacked Chl as is the case
 522 of the cyanobacterial D2_{mod} described here.

523

524 MATERIALS AND METHODS

525 Construction and cultivation of the strains

526 The *Synechocystis* strain expressing exclusively the His-tagged version of D2 and lacking CP47
 527 (His-D2/ Δ CP47) was derived from the Tol145 mutant lacking both copies of D2 as described by
 528 Tang et al. (1993). Plasmid pDC074 carrying a kanamycin-resistance cassette was used as the
 529 parental vector for D2 mutagenesis (Suzuki et al., 2013). The coding sequence of 6xHis tag
 530 (CATCATCATCATCAT) was introduced after the start codon of *psbD1* gene by overlap
 531 extension PCR using the primer set *psbDC1F/psbD-His-2R* and *psbD-His-3F/psbDC4R*
 532 (Supplemental Table S5). The plasmid was then used to transform the Tol145 strain to yield the
 533 His-D2 mutant. Then the *psbB* gene was disrupted using the *pPsbB-GentA* vector where the *psbB*
 534 (*slr0906*) was replaced with gentamycin-resistance cassette oriented as the *slr0906* gene. First, an
 535 intermediate vector, namely pGEMT-*psbB*, was constructed via overlap extension PCR. Primer
 536 sets *slr0906-1F/slr0906-2R* and *slr0906-3F/slr0906-4R* (Supplemental Table S5) were used to
 537 amplify the upstream and downstream flanking sequences, respectively. Both upstream and
 538 downstream fragments were then mixed as the DNA template for overlap extension reaction

539 using the primers *slr0906*-1F and *slr0906*-4R. The resulting fragments, which carry an *EcoRV*
540 restriction site instead of *slr0906*, were then cloned into the multiple cloning region of the
541 pGEM-T Easy vector. Further modifications were then carried out by inserting a gentamycin-
542 resistance cassette into the *EcoRV* site via restriction digestion and ligation to create the final
543 transformation vector p*PsbB*-GentA. To disrupt the *ycf39* locus in the His-D2/ Δ CP47 mutant we
544 used the transformation vector p*Slr0399*-ErmA as in Knoppová et al. (2014). The genotypes of
545 the mutants were confirmed by PCR and sequencing. The CP47-less strain Δ CP47 (Eaton-Rye
546 and Vermaas, 1991) was used as a control strain for the evaluation of RCII level (Fig. S1) and for
547 the purification of proteins using the Ni-affinity chromatography (Fig. S7).

548 The strain expressing the C-terminal FLAG-tagged variant of the PsbI subunit and lacking CP47
549 (PsbI-FLAG/ Δ CP47) was obtained by transforming the CP47 deletion mutant (Eaton-Rye and
550 Vermaas, 1991) using a synthetic DNA construct (Genscript, USA) in which the 3xFLAG coding
551 sequence (Sigma) was inserted before the *psbI* STOP codon and an erythromycin-resistance
552 cassette downstream the gene was used as a selection marker. The Ycf39-binding RCII* was
553 isolated from the CP47-less strain expressing FLAG-Ycf39 as described in Knoppová et al.
554 (2014). The PSII-lacking strains expressing either FLAG-D1 or FLAG-D2 were based on the
555 PSII-less strain Δ D1/ Δ D2/ Δ CP43/ Δ CP47 (Trinugroho et al., 2020) where the N-terminal FLAG-
556 tagged versions of D1 or D2 proteins were introduced using the pPD-FLAG vector
557 (Hollingshead et al., 2012). The *psaA/psaB* deletion strain Δ PSI, the *psbEFLJ* deletion strain
558 Δ CYT, the *ftsH2* deletion strain Δ FtsH2 and *phb3* deletion strain Δ Phb3 were described in Shen
559 et al. (1993), Pakrasi et al. (1988), Komenda et al. (2006) and Boehm et al. (2009), respectively.
560 The corresponding multiple deletion mutants were obtained by transformation using the genomic
561 DNA isolated from these strains.

562 For purification of the RCII, D1 and D2 complexes, 4-L cultures were grown in 10-L round
563 bottomed flasks in BG11 medium supplemented with 5 mM glucose at 30°C at a surface
564 irradiance of 100 $\mu\text{mol photons m}^{-2} \text{s}^{-1}$. The culture was agitated using a magnetic stirrer and
565 bubbled with air. For thylakoid membrane protein analyses, the strains were grown in 100 mL of
566 BG11 medium plus 5 mM glucose using 250 mL conical flasks on a rotary shaker under 40 μmol
567 $\text{photons m}^{-2} \text{s}^{-1}$ at 28°C.

568 **Isolation of thylakoid membranes and tag-specific purification**

569 Thylakoid membranes were isolated in buffer A (25 mM MES/NaOH, pH 6.5, 10 mM CaCl₂, 10
570 mM MgCl₂, 25% (v/v) glycerol) containing EDTA-free protease inhibitor cocktail (Sigma-
571 Aldrich, USA) using a procedure described in Chidgey et al. (2014). His-tagged RCII was
572 purified using Protino Ni-NTA agarose (MACHEREY-NAGEL, Germany) in a gravity-flow
573 chromatography column at 10 °C after membrane solubilization with DM as described in
574 Knoppová et al. (2021). The FLAG-affinity purification was performed as in Koskela et al.
575 (2020).

576 **Radioactive Labeling**

577 Radioactive pulse and pulse-chase labeling of the cells was performed at 500 μmol photons m⁻² s⁻¹
578 and 30°C using a mixture of [³⁵S]Met and [³⁵S]Cys (Hartmann Analytic GmbH, Braunschweig,
579 Germany) as described in Dobáková et al. (2009).

580 **Protein analyses**

581 The composition of purified complexes was analyzed using two-dimensional system combining
582 CN electrophoresis in a 4 % to 14 % (w/v) gradient polyacrylamide gel with SDS-PAGE in a
583 denaturing 16 % to 20 % (w/v) gradient gel containing 7 M urea (Komenda et al., 2012a). The
584 amount of the pull-down preparation loaded onto the gel corresponded to 0.5 μg of Chl. The first-
585 dimensional native gels were photographed (1D color) and scanned for fluorescence (1D fluo).
586 The proteins separated using the denaturing SDS gels were visualized by staining with either
587 Coomassie Blue (CBB) or SYPRO Orange and detected by MS or immunoblotting. The primary
588 antibodies against D1, D2, CP47, CP43, PsbE and PsbF used in this study were previously
589 described by Komenda et al. (2004) and Dobáková et al. (2007). The antibody against
590 *Synechocystis* Slr0575 and PsbN were raised in rabbit against peptides 161-172 and 32-43 of the
591 *Synechocystis* proteins, respectively, conjugated to keyhole limpet hemocyanin (Moravian
592 Biotechnologies, Czech Republic). We also used our own antibodies raised against *Escherichia*
593 *coli*-expressed Ycf48 (Yu et al., 2018).

594 **Enzymatic digestion and protein identification by mass spectrometry**

595 The CBB-stained protein bands to be identified were cut from the gel and digested by trypsin.
596 Resulting peptides were extracted, purified with ZipTip C18 pipette tips (Millipore, USA) and

597 analyzed using a NanoAcquity UPLC (Waters, USA) on-line coupled to an ESI Q-ToF Premier
598 mass spectrometer (Waters, USA) as described in detail in Janouškovec et al. (2013).
599 The proteins in whole preparations were analyzed after their acetone precipitation. 50 µl of
600 acetone cooled to -20°C was added to the whole protein fraction and after one hour of incubation
601 at -20°C sample was spun down for 10 min at 20 000 g and 4°C. Supernatant was removed and
602 the rest of the acetone was evaporated in a fume hood for approx. 30 minutes. The precipitate was
603 dissolved in 10 µl of 40 mM ammonium bicarbonate in 9 % (v/v) acetonitrile containing 0.4 mg
604 trypsin (proteomics grade; Sigma-Aldrich, USA) and incubated at 37°C overnight. Excessive
605 liquid was removed by Speedvac, and 40 µl of solvent A (0.1 % (v/v) formic acid in water) was
606 added to the 10 µl of tryptic digest. MS analysis was performed using a NanoElute UHPLC
607 (Bruker) on-line coupled to the ESI Q-ToF a high-resolution mass spectrometer (Bruker Impact
608 HD). Peptides were separated by UHPLC using Thermo Trap Cartridge as a trap column and
609 Bruker Fifteen C18 analytical column (75 mm i.d. 150 mm length, particle size 1.9 mm, reverse
610 phase; Bruker). The linear gradient elution ranged from 95 % solvent A (0.1 % (v/v) formic acid
611 in water) to 95 % solvent B (0.1 % (v/v) formic acid in acetonitrile and water (90/10)) at a flow
612 rate of 0.3 mL/min and time 60 min. Eluted peptides flowed directly into the ESI source. Raw
613 data were acquired in the Dynamic MS/MS Spectra Acquisition with following settings: dry
614 temperature 150 °C, drying gas flow 3 l/min, capillary voltage 1300 V, and endplate offset 500
615 V. The spectra were collected in the range 150–2000 m/z with spectra rate 2 Hz. The CID was set
616 as a ramp from 20 to 60 eV on masses 200–1200, respectively. The acquired spectra were
617 submitted for database search using the MaxQuant software against *Synechocystis* protein
618 databases from the Uniprot Web site (<https://www.uniprot.org/proteomes/UP000001425>). Acetyl
619 N-terminal, deamidation N and Q, carbamidomethyl C, and oxidation M were set as variable
620 modifications. Identification of three consecutive y-ions or b-ions was required for a positive
621 peptide match.

622 **Determination of pigment content**

623 Chl content per cell was determined after methanol extraction of pigments according to Ritchie
624 (2006). The ratio of Chl, Pheo and β-car for a single RCII (one heme-*b*) was determined
625 essentially as described in Trinugroho et al. (2020).

626 **Light-induced charge separation in RCII**

627 Measurements of charge separation activity in the preparation of RCII were performed using a
628 home-built kinetic photodiode array spectrophotometer with side illumination (maximum at 660
629 nm, 1000 $\mu\text{mol photons m}^{-2} \text{s}^{-1}$, provided by an LED source M660L3-C1; Thorlabs, USA)
630 described in Bína et al. (2006). The measurement was performed as described in Vácha et al.
631 (2002). Briefly, samples were diluted to a final Chl concentration of 5 $\mu\text{g ml}^{-1}$ in a buffer A
632 containing 0.04 % (w/v) DM and light-induced oxidation of primary donor was measured in the
633 presence of silicomolybdate at a concentration of 200 μM . Light-induced Pheo reduction was
634 measured in the presence of sodium dithionite and methylviologen at concentrations of 1 mg ml^{-1}
635 and 10 μM , respectively.

636

637 **Accession Numbers**

638 The Uniprot database accession numbers of proteins identified in this article can be found in
639 Table 2, Supplemental Figure S7 and Supplemental Tables S1, S2, S3, and S4.

640

641 **Supplemental Data**

642 Supplemental Figure S1. Two-dimensional protein analysis of membranes isolated from the
643 CP47-less mutant expressing a native or a His-tagged variant of the D2 protein (ΔCP47 and His-
644 D2/ ΔCP47 , respectively).

645 Supplemental Figure S2. Two-dimensional protein analysis of the FLAG-Ycf39 preparation
646 isolated from the CP47-null mutant expressing FLAG-Ycf39.

647 Supplemental Figure S3. Two-dimensional protein analysis of preparations isolated from the
648 CP47-less strains expressing His-tagged D2 protein and lacking Ycf39 (His-D2/ $\Delta\text{CP47}/\Delta\text{Ycf39}$).

649 Supplemental Figure S4. Two-dimensional protein analysis of the membranes isolated from the
650 CP47-less strain (ΔCP47) after the radioactive pulse-labeling (p) followed by 30 and 60 min of
651 the pulse-chase (pch).

652 Supplemental Figure S5. Two-dimensional protein analysis of preparation isolated from the
653 CP47-less strains expressing His-tagged D2 protein.

654 Supplemental Figure S6. Two-dimensional protein analysis of preparations isolated from the
655 CP47-less strains expressing FLAG-tagged PsbI protein using FLAG-specific affinity
656 chromatography.

657 Supplemental Figure S7. Two-dimensional protein analysis of the control preparation isolated by
658 Ni-affinity chromatography from the control CP47-less strains.

659 Supplemental Figure S8. Two-dimensional protein analysis of FLAG-D2 and the control
660 preparation.

661 Supplemental Figure S9. Separation of RCII complexes by ionex chromatography and their
662 absorption spectra.

663 Supplemental Figure S10. Room temperature absorption spectra and 77K chlorophyll
664 fluorescence spectra of the FLAG-D2 and control FLAG-free preparations.

665 Supplemental Figure S11. Two-dimensional protein analysis of radioactively labelled membrane
666 proteins of Δ CP47 and Δ CP47/ Δ Slr0575 strains.

667 Supplemental Figure S12. Native gel analysis of His-D2 preparations isolated from membranes
668 of the CP47-less strain expressing His-D2 solubilized with different concentrations of β -dodecyl-
669 maltoside (DM).

670 Supplemental Figure S13. Two-dimensional protein analysis of preparation isolated from the
671 CP47-less strain lacking FtsH2 and expressing His-tagged D2 protein and the stoichiometry of
672 pigment cofactors in RCII* and RCIIa electrophoretically purified from this preparation.

673 Supplemental Figure S14. Two-dimensional protein analysis of membrane proteins of
674 Δ PSI/ Δ CP47/ Δ CP43 strain.

675 Supplemental Table S1. List of PSII and PSI-related proteins identified by MS and Western
676 blotting in the RCII complexes separated by 2D CN/SDS PAGE from the isolated His-
677 D2/ Δ CP47 preparation (see Fig. 1, arrows) and identification of Slr1470 in the His-D2/ Δ CP47
678 preparation (Fig. S3).

679 Supplemental Table S2. List of the most abundant 40 proteins identified by MS in Flag-
680 PsbI/ Δ CP47 preparation.

681 Supplemental Table S3. List of the most abundant 40 proteins identified by MS in Flag-D1
682 preparation.

683 Supplemental Table S4. List of the most abundant 40 proteins identified by MS in Flag-D2
684 preparation.

685 Supplemental Table S5. List of primers.

686

687 **Funding Information**

688 The work was supported by the Institutional Research Concept (RVO: 61388971), by the Czech
689 Science Foundation (project 19-29225X) and by ERC project Photoredesign (no. 854126). J.Y.,
690 J.P.T. and P.J.N. were supported by the Biotechnology and Biological Sciences Research Council
691 (awards BB/L003260/1 and BB/P00931X/1) and J.P.T. by a PhD scholarship from the Indonesia
692 Endowment Fund for Education (LPDP). D.B. acknowledges Ministry of Education, Youth and
693 Sports of the Czech Republic (project CZ.02.1.01/0.0/0.0/15_003/0000336 (KOROLID)) and
694 Institutional Research Concept (RVO: 60077344).

695

696

697 **Acknowledgments**

698 We thank Eva Prachová, Lucie Kovářová and Jana Zahradníková for excellent technical
699 assistance.

700

701

702 **Tables**

703 **Table 1. The stoichiometry of pigment cofactors present in the crude His-D2 preparation**
704 **and in the RCII*, RCIIa, and PSI/RCIIa complexes.** The complexes were purified from the
705 His-D2/ Δ CP47 strain using a combination of Ni affinity chromatography and native gel
706 electrophoresis. The ratio of all pigments is normalized to one heme. Data shown as mean of
707 three independent replicates; see methods for details of pigment quantification.

708

| Preparation | Stoichiometry of pigment cofactors | | | |
|----------------------|---|---------------------------------|----------------------------------|----------------------|
| | Chl-<i>a</i> | β-car | Pheo | Heme-<i>b</i> |
| Crude His-D2 | 9.7 \pm 2.2 | 2.4 \pm 0.4 | 1.2 \pm 0.3 | 1.0 |
| RCII* | 9.8 \pm 1.1 | 2.6 \pm 0.6 | 1.8 \pm 0.1 | 1.0 |
| RCIIa | 6.7 \pm 0.25 | 1.4 \pm 0.3 | 1.8 \pm 0.05 | 1.0 |
| RCIIa/ PSI(1) | 65.2 \pm 0.7 | 7.5 \pm 1.2 | 1.9 \pm 0.3 | 1.0 |

709

710

711 **Table 2. List of proteins identified by MS specifically in the isolated FLAG-D1/ Δ PSII and**
 712 **FLAG-D2/ Δ PSII preparation after subtraction of proteins identified in the Δ PSII control.**
 713

| Preparation | Protein UniProt KB No. | Mass spectrometric analysis | | | |
|----------------|---------------------------|-----------------------------|--------------|--------------------------|-----------------|
| | | Size (Da) Length (AA) | Coverage (%) | Detected no. of peptides | Intensity |
| FLAG-D1 | Ycf48 P73069 | 37267 342 | 70 | 15 | 54533000 |
| | D1 P16033 | 39695 360 | 29 | 10 | 26748000 |
| | Ycf39 P74429 | 36496 326 | 29 | 10 | 19328000 |
| | Phb3 P72665 | 35727 321 | 61 | 18 | 17022000 |
| FLAG-D2 | | | | | |
| | D2 P09192 | 39466 352 | 21 | 5 | 33302000 |
| | PsbE P09190 | 9442 81 | 26 | 2 | 18318000 |
| | PsbY P73676 | 4202 39 | 21 | 1 | 2790100 |
| | FtsH2 Q55700 | 68496 627 | 47 | 5 | 563000 |
| | Phb3 P72665 | 35727 321 | 12 | 4 | 515600 |
| | FtsH3 P72991 | 67250 616 | 8 | 4 | 353700 |
| | PsbF P09191 | 4929 44 | 39 | 1 | 306100 |
| | Slr1470 P74154 | 14902 131 | 7 | 1 | 182100 |
| | CyanoP P73952 | 20747 188 | 5 | 1 | 51900 |

714 **The analysis of proteins precipitated from the preparation was performed using NanoElute UHPLC**
 715 **(Bruker) on-line coupled to a high-resolution mass spectrometer (Bruker Impact HD).**

716 **Figure Legends**

717 **Fig. 1. Isolation and analysis of RCII complexes.** Room temperature absorption spectra (A), 77
718 K chlorophyll fluorescence spectra (B) and 2D gel analysis of RCII preparation (C) isolated from
719 cells of the CP47-less strain expressing His-tagged D2. The preparation was isolated using Ni
720 affinity chromatography and analyzed using CN PAGE in the first dimension. The native gel was
721 photographed (1D color) and scanned by LAS 4000 for fluorescence (1D fluor). After SDS-
722 PAGE in the 2nd dimension, the gels were stained by SYPRO Orange (2D SYPRO stain). RCII*
723 is the D1-D2 complex containing Ycf39/Hlips, RCIIa and RCIIa(2) are monomeric and dimeric
724 forms of the D1/D2 complex lacking the Ycf39/Hlips complex, respectively, and RCIIa/PSI
725 designates the PSI monomer bound to RCIIa. Designated proteins were identified by mass
726 spectrometry (see Table S1); non-specifically interacting proteins are designated with an asterisk.
727 PsbN and Slr0575 were identified using specific antibodies. 0.5 μg of Chl was loaded onto the
728 gel.

729
730 **Fig. 2. Photochemical activity of RCII complexes.** The light-induced accumulation of P680^+
731 (A) and Pheo^- (B) in two preparations isolated from the CP47-less strain expressing His-tagged
732 D2 protein. The preparations differed in the content of PSI (green circles, sample analyzed in Fig.
733 1C; red squares, sample analyzed in Fig. S5), and in a pea 5-Chl reaction center complex isolated
734 using Cu affinity chromatography (black diamonds). Accumulation of P680^+ (A) and Pheo^- (B)
735 was elicited by strong red actinic light (wavelength 660 nm, $1000 \mu\text{mol photons m}^{-2} \text{s}^{-1}$) in the
736 presence of silicomolybdate (electron acceptor) or sodium dithionite (electron donor),
737 respectively. The curves were normalized to the same absorption value of the preparations at the
738 red Qy absorption maximum of Chl.

739
740 **Fig. 3. Spectroscopic analysis of RCII complexes.** Room temperature absorption spectra (A)
741 and 77 K chlorophyll fluorescence spectra (B) of RCIIa/PSI, RCII* and RCIIa complexes. CN
742 gel electrophoresis was used to purify complexes from the preparation isolated using Ni affinity
743 chromatography from cells of the CP47-less strain expressing the His-tagged D2 protein. The
744 absorption spectra were normalized to the 415 nm maximum and the fluorescence spectra to the
745 680 nm maximum.

746

747 **Fig. 4. HPLC analysis of pigments and heme in the RCII complexes.** RCII* and RCIIa
748 complexes (A) were purified by CN PAGE from the His-D2 preparation and FLAG-D1 and
749 FLAG-D2 preparations (B) were isolated using FLAG affinity chromatography from strains
750 lacking PSII Chl-binding subunits and expressing either FLAG-D1 or FLAG-D2. The analysis
751 was performed as described in Materials and methods and the chromatograms were normalized to
752 the highest peak in the preparation; in RCII*, RCIIa and FLAG-D1 to Chl; in FLAG-D2 to heme.

753
754 **Fig. 5. Spectroscopic analysis of FLAG-D1 and FLAG-D2.** Room temperature absorption
755 spectra (A) and 77 K chlorophyll fluorescence spectra (B) of FLAG-D1 and FLAG-D2. The
756 preparations were isolated using FLAG affinity chromatography from strains lacking PSII Chl-
757 binding subunits and expressing either FLAG-D1 or FLAG-D2. The absorption spectra were
758 normalized to blue maxima, while measurements of the fluorescence spectra were performed
759 using identical volumes of the obtained preparations.

760
761 **Fig. 6. Two-dimensional protein analysis of FLAG-D1 and FLAG-D2.** The preparations were
762 isolated using FLAG affinity chromatography from strains lacking PSII Chl-binding subunits and
763 expressing either FLAG-D1 (FLAG-D1/ Δ PSII) or FLAG-D2 (FLAG-D2/ Δ PSII). The analysis
764 was performed by CN PAGE in the first dimension and the native gel photographed (1D color)
765 and scanned by LAS 4000 for fluorescence (1D fluor). Following SDS-PAGE in the 2nd
766 dimension, the gel was scanned for Chl fluorescence (Chl, 2D fluor), then stained by SYPRO
767 Orange (2D SYPRO stain) and probed with the designated antibodies (2D blots). Blue arrows
768 mark the fastest native forms of FLAG-D1 (F.D1) and FLAG-D2 (F.D2) and red arrows their Chl
769 fluorescence signals. Chl fluorescence of slower F.D1 and F.D2 forms is in a red dashed
770 rectangle. FP designates free pigments. Both preparations were isolated from the same amount of
771 cells and the analysis was performed on identical volumes of the obtained preparations.

772
773

- 774
775 **References**
- 776 **Barber J** (2014) Photosystem II: Its function, structure, and implications for artificial
777 photosynthesis. *Biochemistry-Moscow* **79**: 185-196
- 778 **Bína D, Litvín R, Vácha F, Šiffel P** (2006) New multichannel kinetic spectrophotometer–
779 fluorimeter with pulsed measuring beam for photosynthesis research. *Photosynthesis Res*
780 **88**: 351-356
- 781 **Boehm M, Nield J, Zhang PP, Aro EM, Komenda J, Nixon PJ** (2009) Structural and
782 mutational analysis of band 7 proteins in the cyanobacterium *Synechocystis* sp strain PCC
783 6803. *J Bacteriol* **191**: 6425-6435
- 784 **Boehm M, Romero E, Reisinger V, Yu J, Komenda J, Eichacker LA, Dekker JP, Nixon PJ**
785 (2011) Investigating the early stages of Photosystem II assembly in *Synechocystis* sp.
786 PCC 6803 isolation of CP47 and CP43 complexes. *J Biol Chem* **286**: 14812-14819
- 787 **Boehm M, Yu J, Reisinger V, Bečková M, Eichacker LA, Schlodder E, Komenda J, Nixon**
788 **PJ** (2012) Subunit composition of CP43-less photosystem II complexes of *Synechocystis*
789 sp. PCC 6803: implications for the assembly and repair of photosystem II. *Philos Trans R*
790 *Soc Ser B: Biol Sci* **367**: 3444-3454
- 791 **Bučinská L, Kiss E, Koník P, Knoppová J, Komenda J, Sobotka R** (2018) The ribosome-
792 bound protein Pam68 promotes insertion of chlorophyll into the CP47 subunit of
793 photosystem II. *Plant Physiol* **176**: 2931-2942
- 794 **Chidgey JW, Linhartová M, Komenda J, Jackson PJ, Dickman MJ, Canniffe DP, Koník P,**
795 **Pilný J, Hunter CN, Sobotka R** (2014) A cyanobacterial chlorophyll synthase-HliD
796 complex associates with the Ycf39 protein and the YidC/Alb3 insertase. *Plant Cell* **26**:
797 1267-1279
- 798 **Cormann KU, Bartsch M, Rögner M, Nowaczyk MM** (2014) Localization of the CyanoP
799 binding site on photosystem II by surface plasmon resonance spectroscopy. *Front Plant*
800 *Sci* **5**
- 801 **Diner BA, Rappaport F** (2002) Structure, dynamics, and energetics of the primary
802 photochemistry of photosystem II of oxygenic photosynthesis. *Ann Rev Plant Biol* **53**:
803 551-580

804 **Dobáková M, Sobotka R, Tichý M, Komenda J** (2009) Psb28 protein is involved in the
805 biogenesis of the photosystem II inner antenna CP47 (PsbB) in the cyanobacterium
806 *Synechocystis* sp. PCC 6803. *Plant Physiol* **149**: 1076-1086

807 **Dobáková M, Tichý M, Komenda J** (2007) Role of the PsbI protein in photosystem II assembly
808 and repair in the cyanobacterium *Synechocystis* sp PCC 6803. *Plant Physiol* **145**: 1681-
809 1691

810 **Eaton-Rye JJ, Vermaas WF** (1991) Oligonucleotide-directed mutagenesis of psbB, the gene
811 encoding CP47, employing a deletion mutant strain of the cyanobacterium *Synechocystis*
812 sp. PCC 6803. *Plant Mol Biol* **17**: 1165-1177

813 **García-Cerdán JG, Furst AL, McDonald KL, Schünemann D, Francis MB, Niyogi KK**
814 (2019) A thylakoid membrane-bound and redox-active rubredoxin (RBD1) functions in
815 de novo assembly and repair of photosystem II. *Proc Natl Acad Sci USA* **116**: 16631-
816 16640

817 **Giorgi LB, Nixon PJ, Merry SAP, Joseph DM, Durrant JR, Rivas JDL, Barber J, Porter G,**
818 **Klug DR** (1996) Comparison of primary charge separation in the photosystem II reaction
819 center complex isolated from wild-type and D1-130 mutants of the cyanobacterium
820 *Synechocystis* PCC 6803. *J Biol Chem* **271**: 2093-2101

821 **Gisriel CJ, Zhou KF, Huang HL, Debus RJ, Xiong Y, Brudvig GW** (2020) Cryo-EM
822 structure of monomeric photosystem II from *Synechocystis* sp. PCC 6803 lacking the
823 water-oxidation complex. *Joule* **4**: 2131-2148

824 **Gounaris K, Chapman DJ, Barber J** (1989) Isolation and characterisation of a
825 D1/D2/cytochrome b-559 complex from *Synechocystis* 6803. *Biochim Biophys Acta* **973**:
826 296-301

827 **Gounaris K, Chapman DJ, Booth P, Crystall B, Giorgi LB, Klug DR, Porter G, Barber J**
828 (1990) Comparison of the D1/D2/cytochrome-b559 reaction center complex of
829 photosystem two isolated by two different methods. *FEBS Lett* **265**: 88-92

830 **Guskov A, Kern J, Gabdulkhakov A, Broser M, Zouni A, Saenger W** (2009) Cyanobacterial
831 photosystem II at 2.9-Å resolution and the role of quinones, lipids, channels and chloride.
832 *Nat Struct Mol Biol* **16**: 334-342

833 **Heinz S, Liauw P, Nickelsen J, Nowaczyk M** (2016) Analysis of photosystem II biogenesis in
834 cyanobacteria. *Biochim Biophys Acta* **1857**: 274-287

- 835 **Hey D, Grimm B** (2018) ONE-HELIX PROTEIN2 (OHP2) is required for the stability of OHP1
836 and assembly factor HCF244 and is functionally linked to PSII biogenesis. *Plant Physiol*
837 **177**: 1453-1472
- 838 **Hollingshead S, Kopečná J, Armstrong DR, Bučinská L, Jackson PJ, Chen GE, Dickman**
839 **MJ, Williamson MP, Sobotka R, Hunter CN** (2016) Synthesis of chlorophyll-binding
840 proteins in a fully segregated $\Delta ycf54$ strain of the cyanobacterium *Synechocystis* PCC
841 6803. *Front Plant Sci* **7**
- 842 **Hollingshead S, Kopečná J, Jackson PJ, Canniffe DP, Davison PA, Dickman MJ, Sobotka**
843 **R, Hunter CN** (2012) Conserved chloroplast open-reading frame *ycf54* is required for
844 activity of the magnesium protoporphyrin monomethylester oxidative cyclase in
845 *Synechocystis* PCC 6803. *J Biol Chem* **287**: 27823-27833
- 846 **Ifuku K** (2015) Localization and functional characterization of the extrinsic subunits of
847 photosystem II: an update. *Biosci, Biotechnol, Biochem* **79**: 1223-1231
- 848 **Janouškovec J, Sobotka R, Lai DH, Flegontov P, Koník P, Komenda J, Ali S, Prášil O, Pain**
849 **A, Oborník M, et al.** (2013) Split photosystem protein, linear-mapping topology, and
850 growth of structural complexity in the plastid genome of *Chromera velia*. *Mol Biol Evol*
851 **30**: 2447-2462
- 852 **Kato K, Miyazaki N, Hamaguchi T, Nakajima Y, Akita F, Yonekura K, Shen J-R** (2021)
853 High-resolution cryo-EM structure of photosystem II reveals damage from high-dose
854 electron beams. *Commun Biol* **4**: 382
- 855 **Kavanagh K, Jornvall H, Persson B, Oppermann U** (2008) The SDR superfamily: functional
856 and structural diversity within a family of metabolic and regulatory enzymes. *Cell Mol*
857 *Life Sci* **65**: 3895-3906
- 858 **Kiss E, Knoppová J, Aznar GP, Pilný J, Yu J, Halada P, Nixon PJ, Sobotka R, Komenda J**
859 (2019) A photosynthesis-specific rubredoxin-like protein is required for efficient
860 association of the D1 and D2 proteins during the initial steps of photosystem II assembly.
861 *Plant Cell* **31**: 2241-2258
- 862 **Knoppová J, Sobotka R, Tichý M, Yu J, Koník P, Halada P, Nixon PJ, Komenda J** (2014)
863 Discovery of a chlorophyll binding protein complex involved in the early steps of
864 photosystem II assembly in *Synechocystis*. *Plant Cell* **26**: 1200-1212

865 **Knoppová J, Yu JF, Janouškovec J, Halada P, Nixon PJ, Whitelegge JP, Komenda J** (2021)
866 The photosystem II assembly factor Ycf48 from the cyanobacterium *Synechocystis* sp.
867 PCC 6803 is lipidated using an atypical lipobox sequence. *Int J Mol Sci* **22**

868 **Knoppová J, Yu JF, Konik P, Nixon PJ, Komenda J** (2016) CyanoP is involved in the early
869 steps of photosystem II assembly in the cyanobacterium *Synechocystis* sp PCC 6803.
870 *Plant Cell Physiol* **57**: 1921-1931

871 **Komenda J, Barker M, Kuviková S, de Vries R, Mullineaux CW, Tichý M, Nixon PJ** (2006)
872 The FtsH protease slr0228 is important for quality control of photosystem II in the
873 thylakoid membrane of *Synechocystis* sp PCC 6803. *J Biol Chem* **281**: 1145-1151

874 **Komenda J, Knoppová J, Kopečná J, Sobotka R, Halada P, Yu JF, Nickelsen J, Boehm M,**
875 **Nixon PJ** (2012a) The Psb27 assembly factor binds to the CP43 complex of photosystem
876 II in the cyanobacterium *Synechocystis* sp. PCC 6803. *Plant Physiol* **158**: 476-486

877 **Komenda J, Knoppová J, Krynická V, Nixon PJ, Tichý M** (2010) Role of FtsH2 in the repair
878 of photosystem II in mutants of the cyanobacterium *Synechocystis* PCC 6803 with
879 impaired assembly or stability of the CaMn₄ cluster. *Biochim Biophys Acta* **1797**: 566-
880 575

881 **Komenda J, Nickelsen J, Tichý M, Prášil O, Eichacker LA, Nixon PJ** (2008) The
882 cyanobacterial homologue of HCF136/YCF48 is a component of an early photosystem II
883 assembly complex and is important for both the efficient assembly and repair of
884 photosystem II in *Synechocystis* sp PCC 6803. *J Biol Chem* **283**: 22390-22399

885 **Komenda J, Reisinger V, Muller BC, Dobáková M, Granvogl B, Eichacker LA** (2004)
886 Accumulation of the D2 protein is a key regulatory step for assembly of the photosystem
887 II reaction center complex in *Synechocystis* PCC 6803. *J Biol Chem* **279**: 48620-48629

888 **Komenda J, Sobotka R** (2016) Cyanobacterial high-light-inducible proteins - Protectors of
889 chlorophyll-protein synthesis and assembly. *Biochim Biophys Acta* **1857**: 288-295

890 **Komenda J, Sobotka R, Nixon PJ** (2012b) Assembling and maintaining the photosystem II
891 complex in chloroplasts and cyanobacteria. *Curr Opin Plant Biol* **15**: 245-251

892 **Kopečná J, Komenda J, Bučinská L, Sobotka R** (2012) Long-term acclimation of the
893 cyanobacterium *Synechocystis* sp. PCC 6803 to high light is accompanied by an enhanced
894 production of chlorophyll that is preferentially channeled to trimeric photosystem I. *Plant*
895 *Physiol* **160**: 2239-2250

- 896 **Koskela MM, Skotnicová P, Kiss É, Sobotka R** (2020) Purification of protein-complexes from
897 the cyanobacterium *Synechocystis* sp. PCC 6803 using FLAG-affinity chromatography.
898 *Bio-protocol* **10**: e3616
- 899 **Krynická V, Shao S, Nixon PJ, Komenda J** (2015) Accessibility controls selective degradation
900 of photosystem II subunits by FtsH protease. *Nature Plants* **1**: 15168
- 901 **Link S, Meierhoff K, Westhoff P** (2012) The atypical short-chain dehydrogenases HCF173 and
902 HCF244 are jointly involved in translational initiation of the *psbA* mRNA of *Arabidopsis*
903 *thaliana*. *Plant Physiol*: pp.112.205104
- 904 **Lopez D, Koch G** (2017) Exploring functional membrane microdomains in bacteria: an
905 overview. *Cur Opin Microbiol* **36**: 76-84
- 906 **Lu Y** (2016) Identification and roles of photosystem II assembly, stability, and repair factors in
907 *Arabidopsis*. *Front Plant Sci* **7**
- 908 **Malavath T, Caspy I, Netzer-El SY, Klaiman D, Nelson N** (2018) Structure and function of
909 wild-type and subunit-depleted photosystem I in *Synechocystis*. *Biochim Biophys Acta*
910 **1859**: 645-654
- 911 **Mayes SR, Dubbs JM, Vass I, Hideg E, Nagy L, Barber J** (1993) Further characterization of
912 the *psbH* locus of *Synechocystis* sp. PCC 6803: Inactivation of *psbH* impairs QA to QB
913 electron transport in photosystem 2. *Biochemistry* **32**: 1454-1465
- 914 **Muller B, Eichacker LA** (1999) Assembly of the D1 precursor in monomeric photosystem II
915 reaction center precomplexes precedes chlorophyll a-triggered accumulation of reaction
916 center II in barley etioplasts. *Plant Cell* **11**: 2365-2377
- 917 **Myouga F, Takahashi K, Tanaka R, Nagata N, Kiss AZ, Funk C, Nomura Y, Nakagami H,**
918 **Jansson S, Shinozaki K** (2018) Stable accumulation of photosystem II requires ONE-
919 HELIX PROTEIN1 (OHP1) of the light harvesting-like family. *Plant Physiol* **176**: 2277-
920 2291
- 921 **Nanba O, Satoh K** (1987) Isolation of a photosystem-II reaction center consisting of D-1 and D-
922 2 polypeptides and cytochrome-b-559. *Proc Natl Acad Sci USA* **84**: 109-112
- 923 **Nickelsen J, Rengstl B** (2013) Photosystem II assembly: from cyanobacteria to plants. *In* SS
924 Merchant, ed, *Ann Rev Plant Biol*, Vol 64, pp 609-635
- 925 **Nixon PJ, Michoux F, Yu JF, Boehm M, Komenda J** (2010) Recent advances in understanding
926 the assembly and repair of photosystem II. *Ann Bot* **106**: 1-16

- 927 **Oren-Shamir M, Sai PSM, Edelman M, Scherz A** (1995) Isolation and spectroscopic
928 characterization of a plant-like photosystem-II reaction center from the cyanobacterium
929 *Synechocystis* sp. 6803. *Biochemistry* **34**: 5523-5526
- 930 **Pakrasi HB, Williams JGK, Arntzen CJ** (1988) Targeted mutagenesis of the *psbE* and *psbF*
931 genes blocks photosynthetic electron transport: evidence for a functional role of
932 cytochrome *b₅₅₉* in photosystem II. *EMBO J* **7**: 325-332
- 933 **Rast A, Schaffer M, Albert S, Wan W, Pfeffer S, Beck F, Plitzko JM, Nickelsen J, Engel BD**
934 (2019) Biogenic regions of cyanobacterial thylakoids form contact sites with the plasma
935 membrane. *Nat Plants* **5**: 436-446
- 936 **Ritchie RJ** (2006) Consistent sets of spectrophotometric chlorophyll equations for acetone,
937 methanol and ethanol solvents. *Photosynthesis Res* **89**: 27-41
- 938 **Rivera-Milla E, Stuermer CAO, Malaga-Trillo E** (2006) Ancient origin of reggie (flotillin),
939 reggie-like, and other lipid-raft proteins: convergent evolution of the SPFH domain. *Cel*
940 *Mol Life Sci* **63**: 343-357
- 941 **Romero E, Diner Bruce A, Nixon Peter J, Coleman Wiliam J, Dekker Jan P, van Grondelle**
942 **R** (2012) Mixed exciton–charge-transfer states in photosystem II: Stark spectroscopy on
943 site-directed mutants. *Biophys J* **103**: 185-194
- 944 **Roose JL, Frankel LK, Mummadisetti MP, Bricker TM** (2016) The extrinsic proteins of
945 photosystem II: update. *Planta* **243**: 889-908
- 946 **Saikawa N, Akiyama Y, Ito K** (2004) FtsH exists as an exceptionally large complex containing
947 HflKC in the plasma membrane of *Escherichia coli*. *J Struct Biol* **146**: 123-129
- 948 **Schottkowski M, Gkalypoudis S, Tzekova N, Stelljes C, Schunemann D, Ankele E,**
949 **Nickelsen J** (2009) Interaction of the periplasmic PrtA factor and the PsbA (D1) protein
950 during biogenesis of photosystem II in *Synechocystis* sp PCC 6803. *J Biol Chem* **284**:
951 1813-1819
- 952 **Shen GZ, Boussiba S, Vermaas WFJ** (1993) *Synechocystis* sp PCC-6803 strains lacking
953 Photosystem-I and phycobilisome function. *Plant Cell* **5**: 1853-1863
- 954 **Shinopoulos KE, Brudvig GW** (2012) Cytochrome *b₅₅₉* and cyclic electron transfer within
955 photosystem II. *Biochim Biophys Acta* **1817**: 66-75

- 956 **Shukla MK, Llansola-Portoles MJ, Tichý M, Pascal AA, Robert B, Sobotka R** (2018)
957 Binding of pigments to the cyanobacterial high-light-inducible protein HliC.
958 *Photosynthesis Res* **137**: 29-39
- 959 **Staleva H, Komenda J, Shukla MK, Šlouf V, Kaňa R, Polívka T, Sobotka R** (2015)
960 Mechanism of photoprotection in the cyanobacterial ancestor of plant antenna proteins.
961 *Nat Chem Biol* **11**: 287-291
- 962 **Suzuki H, Yu JF, Kobayashi T, Nakanishi H, Nixon PJ, Noguchi T** (2013) Functional roles of
963 D2-Lys317 and the interacting chloride ion in the water oxidation reaction of photosystem
964 II as revealed by Fourier transform infrared analysis. *Biochemistry* **52**: 4748-4757
- 965 **Tang XS, Chisholm DA, Dismukes GC, Brudvig GW, Diner BA** (1993) Spectroscopic
966 Evidence from Site-Directed Mutants of *Synechocystis* PCC6803 in Favor of a Close
967 Interaction between Histidine-189 and Redox-Active Tyrosine-1608 Both of Polypeptide
968 D2 of the Photosystem II Reaction Center. *Biochemistry* **32**: 13742-13748
- 969 **Thompson EP** (2016) Proteins involved in the maintenance of the photosynthetic apparatus in
970 cyanobacteria and plants. Ph.D. thesis. University College London
- 971 **Tomo T, Akimoto S, Tsuchiya T, Fukuya M, Tanaka K, Mimuro M** (2008) Isolation and
972 spectral characterization of photosystem II reaction center from *Synechocystis* sp PCC
973 6803. *Photosynthesis Res* **98**: 293-302
- 974 **Torabi S, Umate P, Manavski N, Plochinger M, Kleinknecht L, Bogireddi H, Herrmann**
975 **RG, Wanner G, Schroder WP, Meurer J** (2014) PsbN is required for assembly of the
976 photosystem II reaction center in *Nicotiana tabacum*. *Plant Cell* **26**: 1183-1199
- 977 **Trinugroho JP, Bečková M, Shao S, Yu J, Zhao Z, Murray JW, Sobotka R, Komenda J,**
978 **Nixon PJ** (2020) Chlorophyll f synthesis by a super-rogue photosystem II complex.
979 *Nature Plants* **6**: 238-244
- 980 **Umena Y, Kawakami K, Shen JR, Kamiya N** (2011) Crystal structure of oxygen-evolving
981 Photosystem II at a resolution of 1.9 Å. *Nature* **473**: 55-60
- 982 **Vácha F, Durchan M, Siffel P** (2002) Excitonic interactions in the reaction centre of
983 photosystem II studied by using circular dichroism. *Biochim Biophys Acta* **1554**: 147-152
- 984 **Walters RG, Shephard F, Rogers JJM, Rolfe SA, Horton P** (2003) Identification of mutants
985 of *Arabidopsis* defective in acclimation of photosynthesis to the light environment. *Plant*
986 *Physiol* **131**: 472-481

- 987 **Xu Q, Bateman A, Finn RD, Abdubek P, Astakhova T, Axelrod HL, Bakolitsa C, Carlton**
988 **D, Chen C, Chiu H-J, et al.** (2010) Bacterial pleckstrin homology domains: A
989 prokaryotic origin for the PH domain. *J Mol Biol* **396**: 31-46
- 990 **Yu JF, Knoppová J, Michoux F, Bialek W, Cota E, Shukla MK, Strašková A, Aznar GP,**
991 **Sobotka R, Komenda J, et al.** (2018) Ycf48 involved in the biogenesis of the oxygen-
992 evolving photosystem II complex is a seven-bladed beta-propeller protein. *Proc Natl Acad*
993 *Sci USA* **115**: E7824-E7833
- 994 **Zouni A, Witt HT, Kern J, Fromme P, Krauss N, Saenger W, Orth P** (2001) Crystal structure
995 of photosystem II from *Synechococcus elongatus* at 3.8 Å resolution. *Nature* **409**: 739-
996 743
- 997

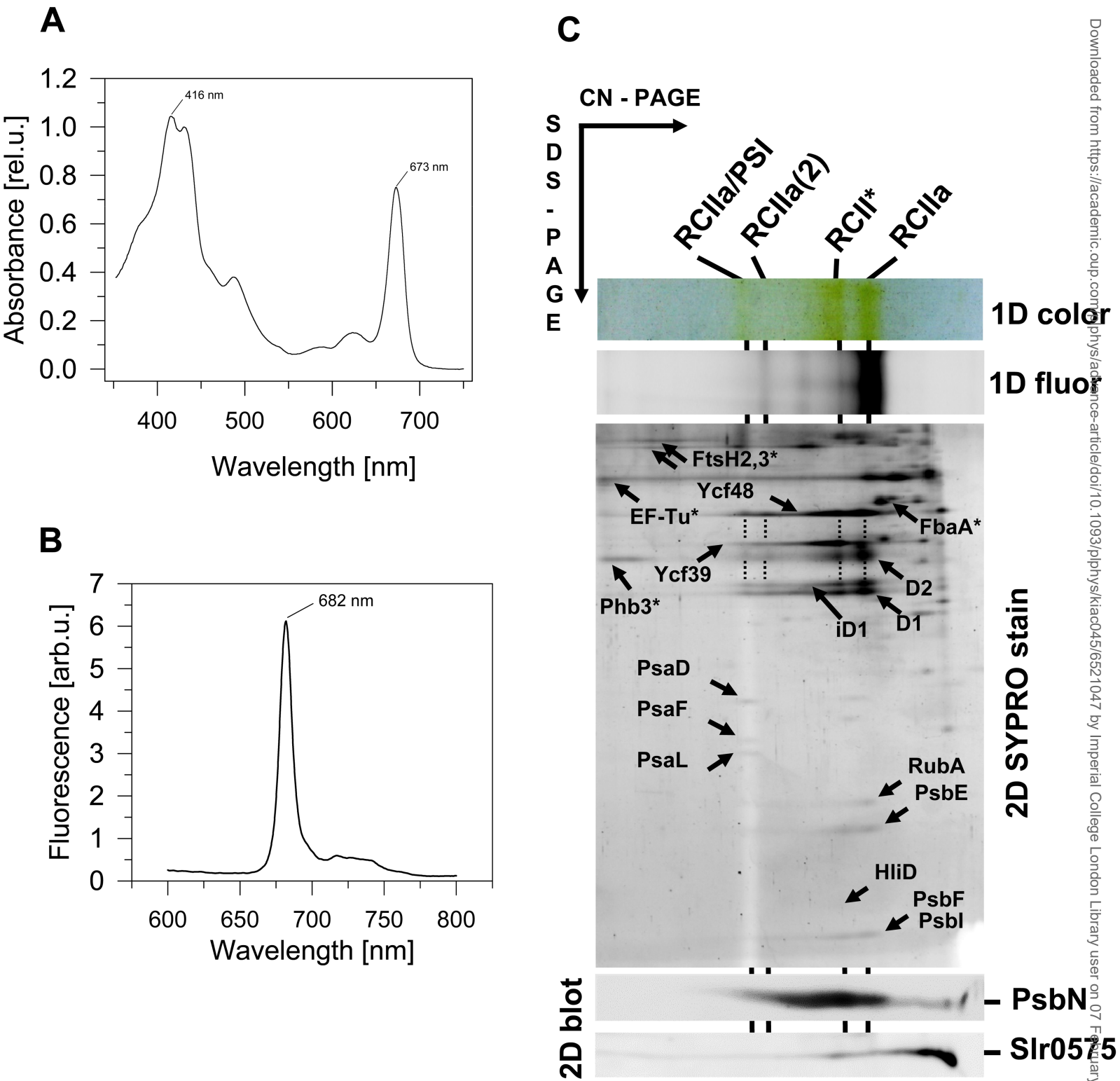
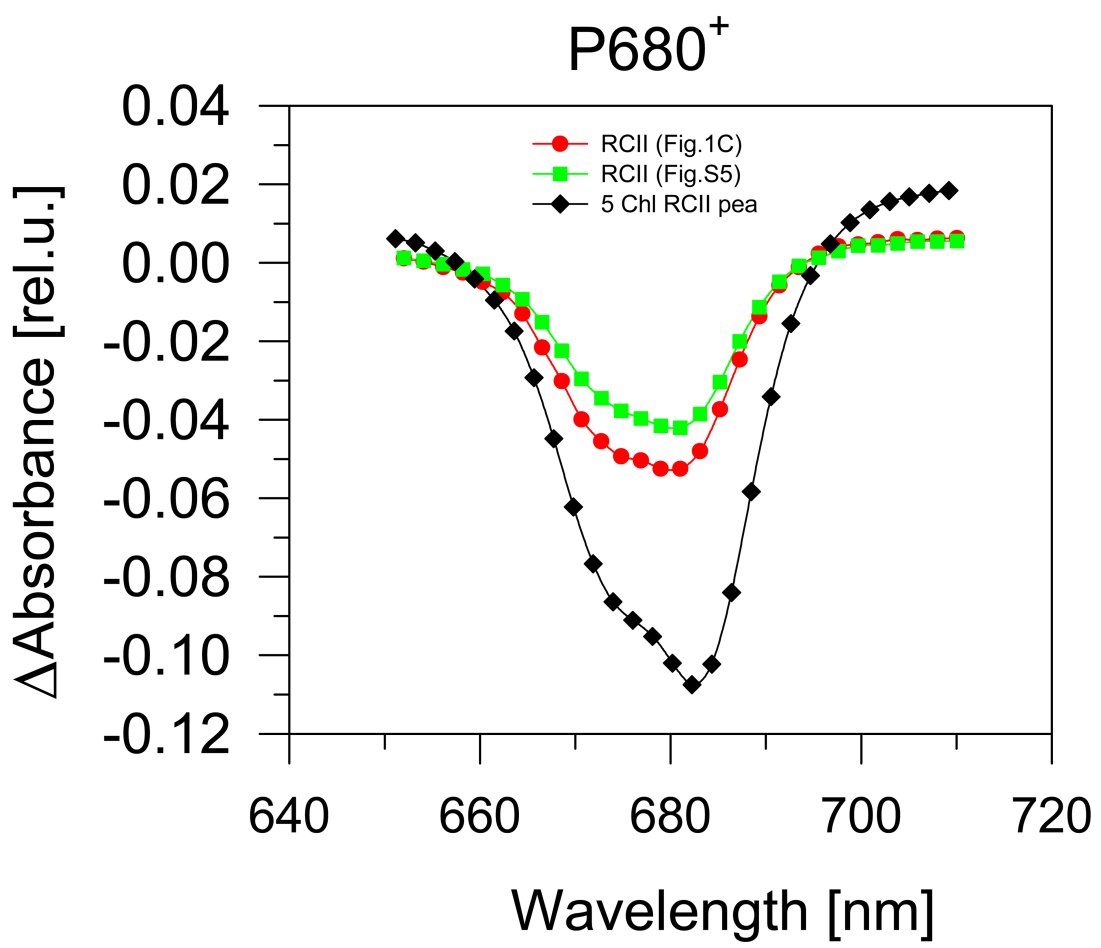
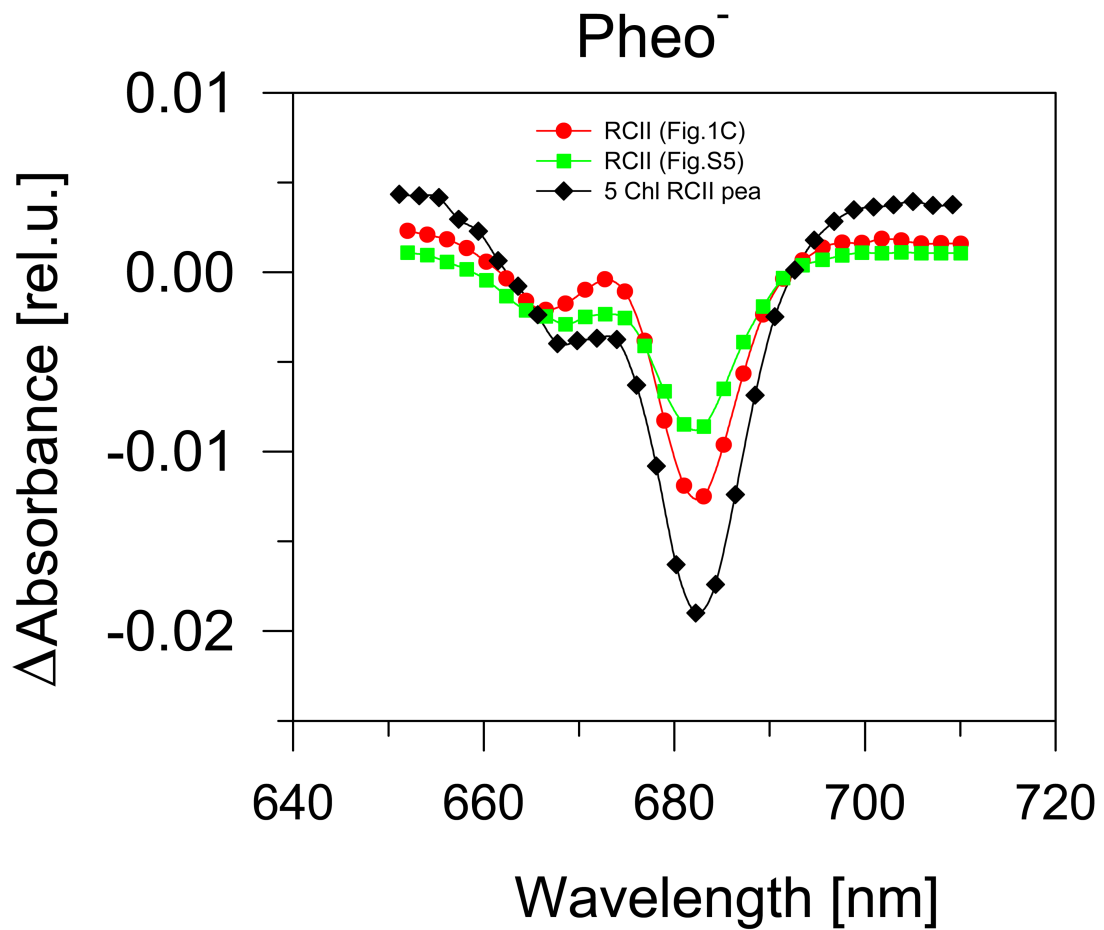
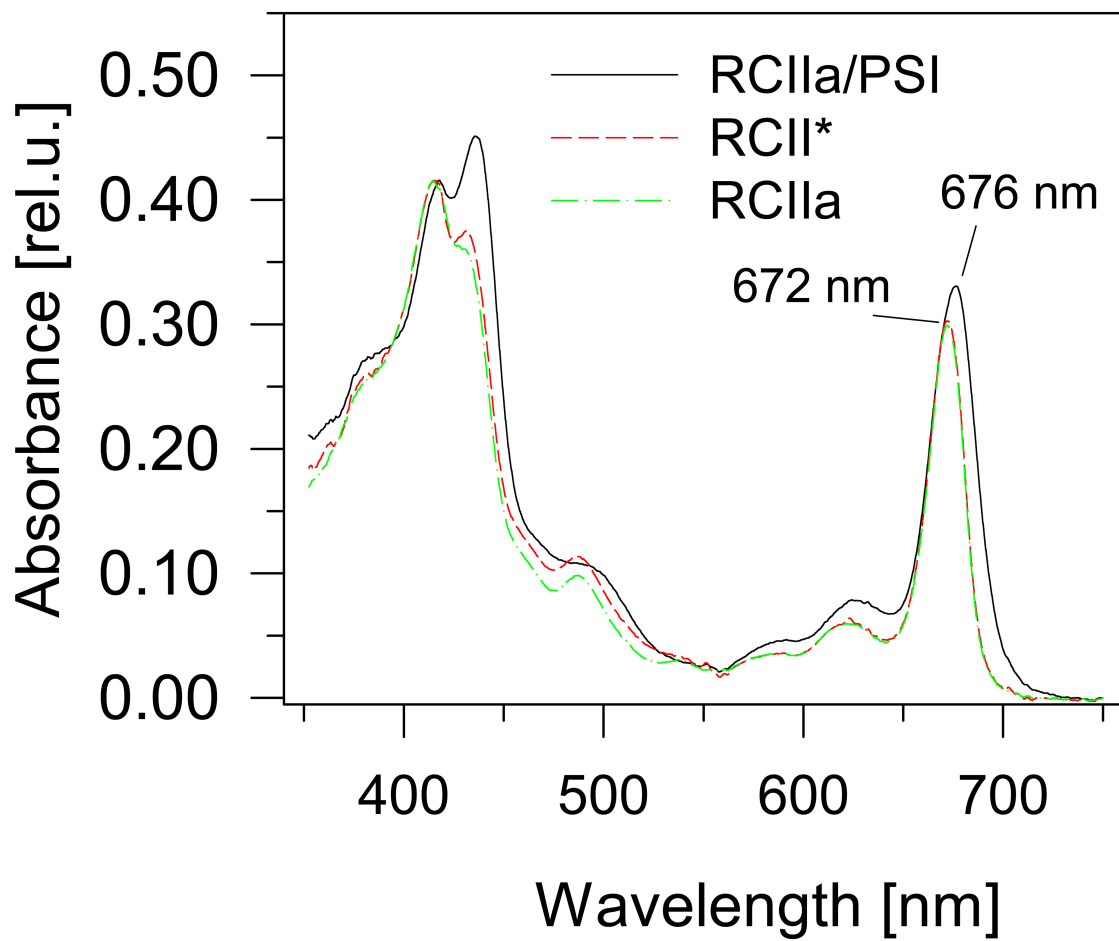
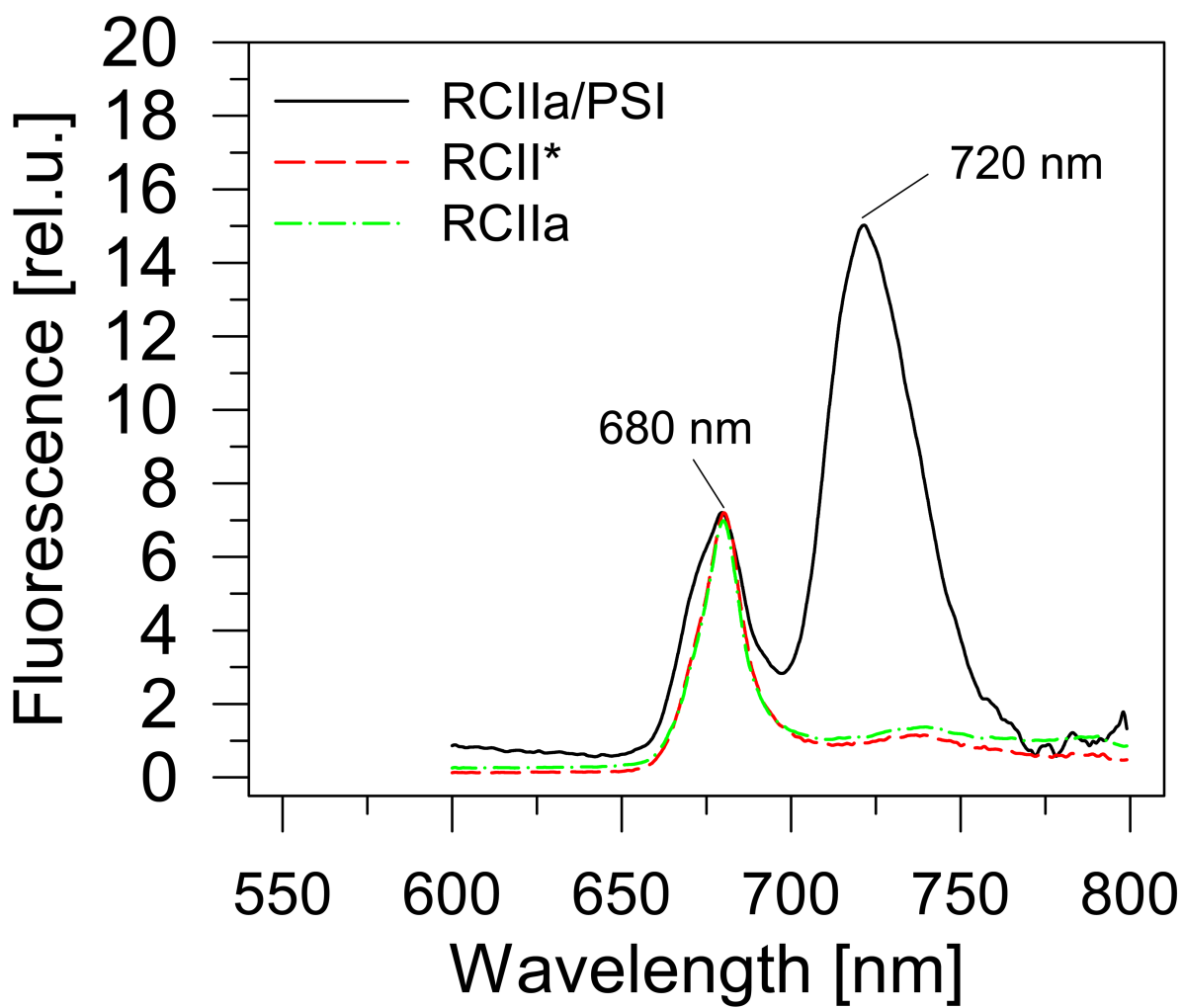
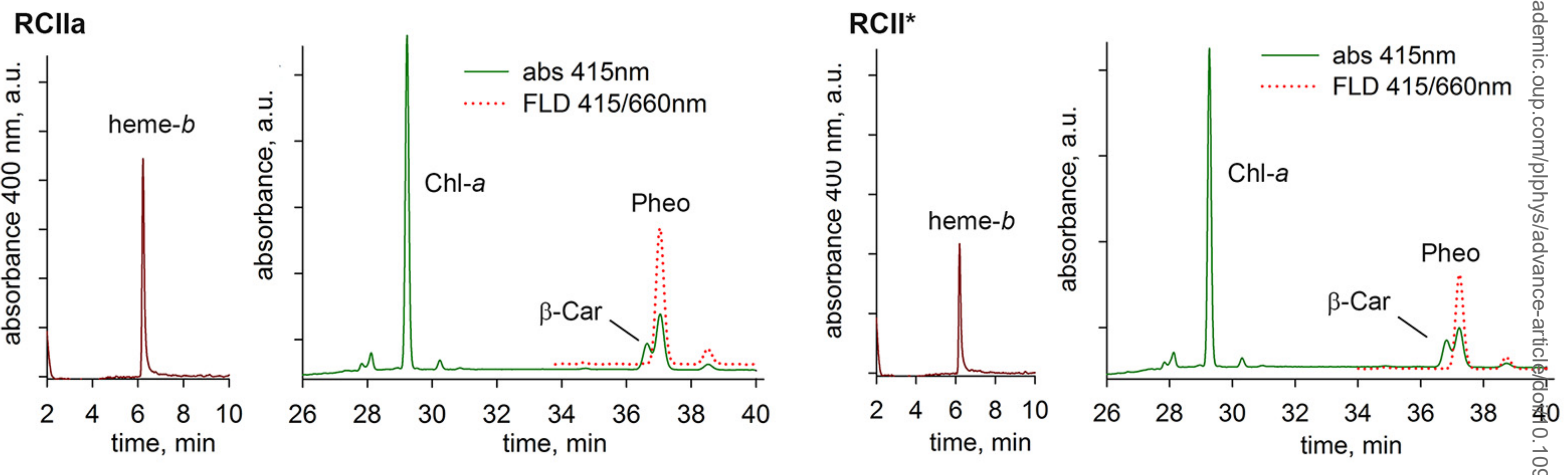


Fig. 1.

A**B****Fig. 2.**

A**B****Fig. 3.**

A



B

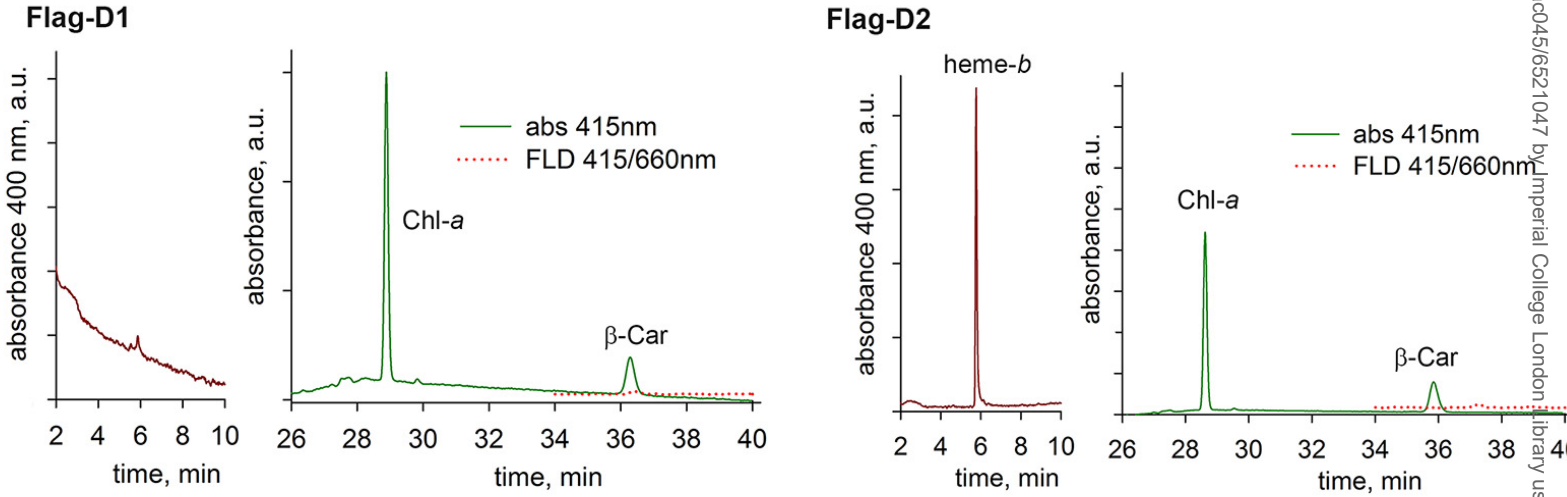
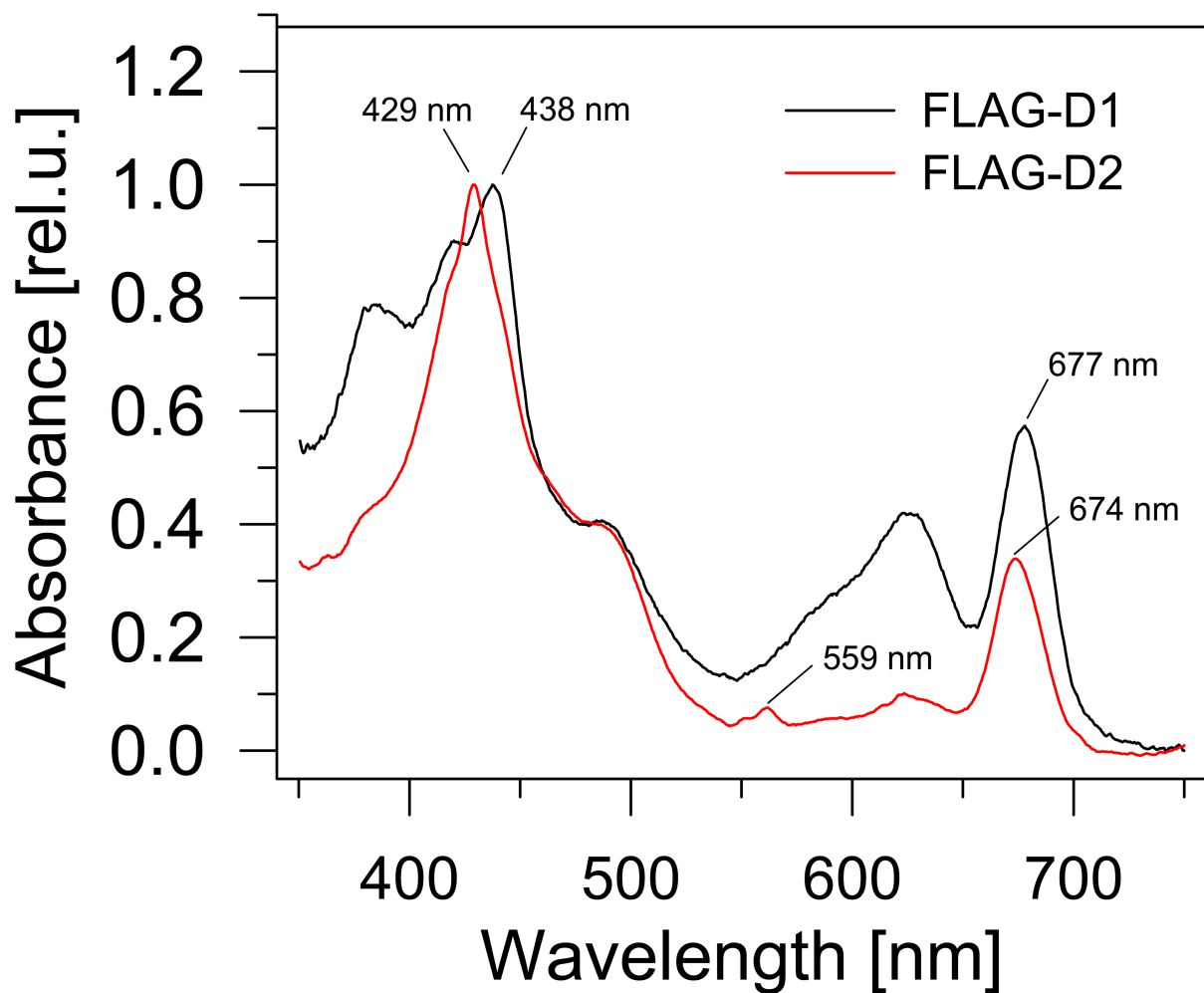


Figure 4.

A



B

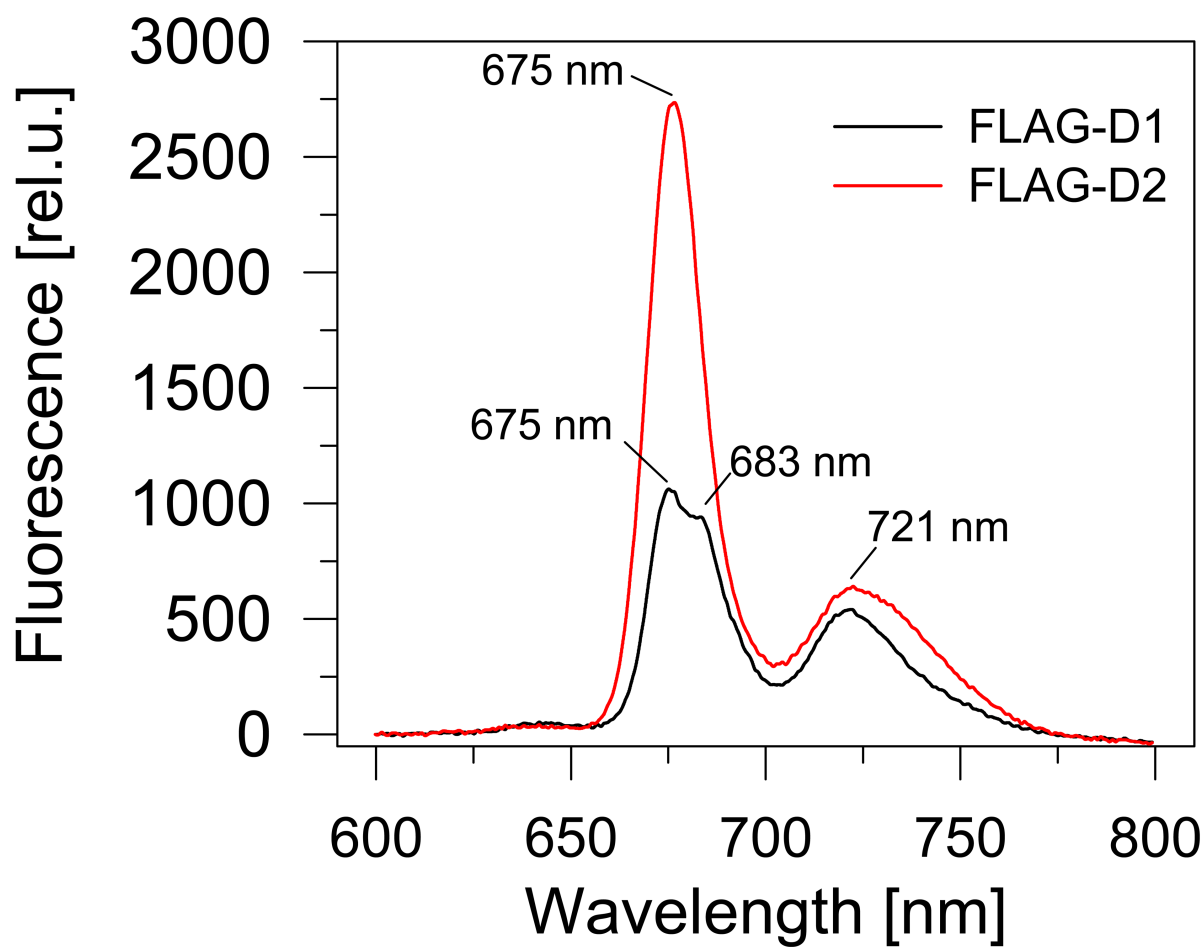


Fig. 5.

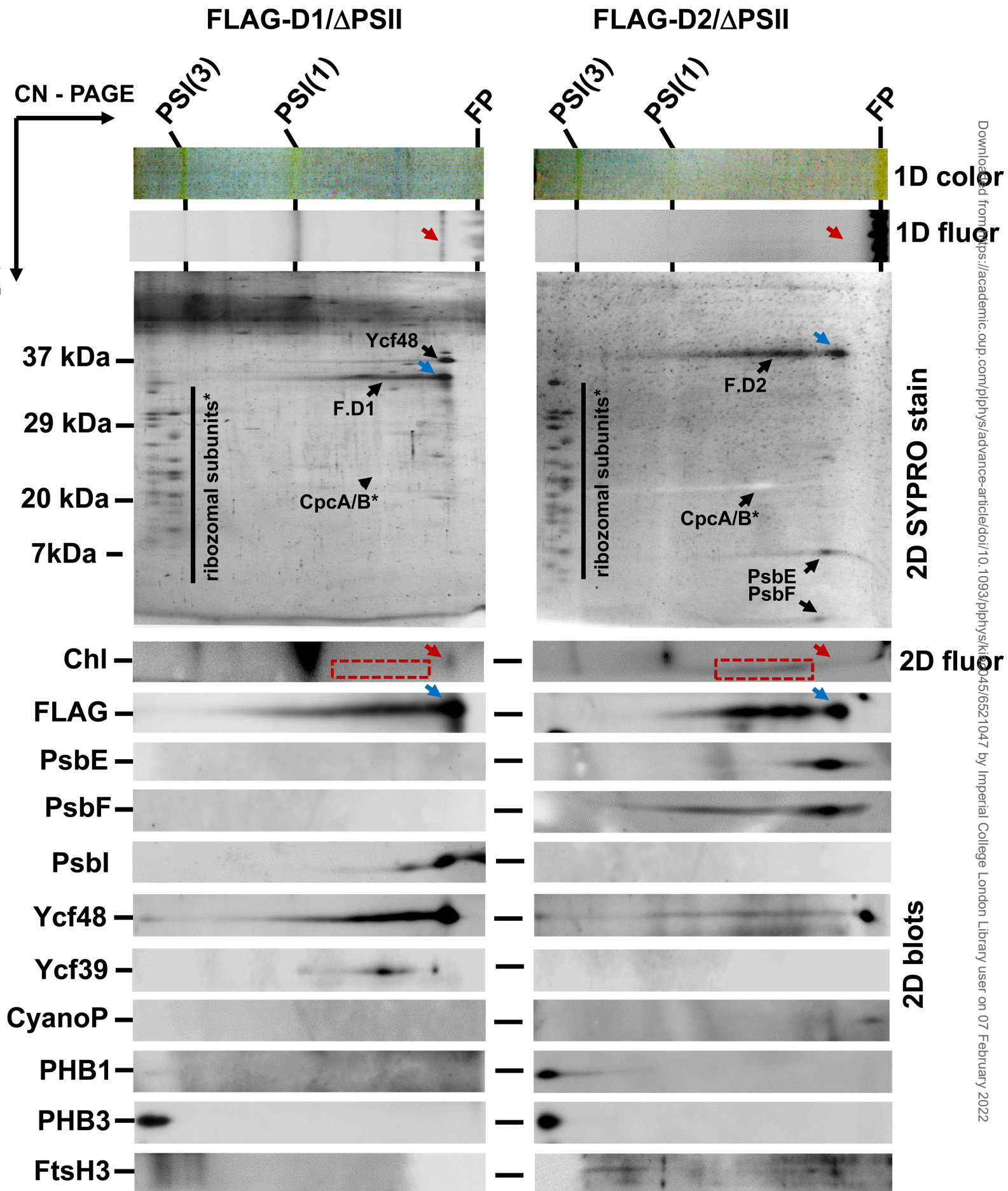


Figure 6.

Parsed Citations

- Barber J (2014) Photosystem II: Its function, structure, and implications for artificial photosynthesis. *Biochemistry-Moscow* 79: 185-196
Google Scholar: [Author Only](#) [Title Only](#) [Author and Title](#)
- Bina D, Litvín R, Vácha F, Šíffel P (2006) New multichannel kinetic spectrophotometer–fluorimeter with pulsed measuring beam for photosynthesis research. *Photosynthesis Res* 88: 351-356
Google Scholar: [Author Only](#) [Title Only](#) [Author and Title](#)
- Boehm M, Nield J, Zhang PP, Aro EM, Komenda J, Nixon PJ (2009) Structural and mutational analysis of band 7 proteins in the cyanobacterium *Synechocystis* sp strain PCC 6803. *J Bacteriol* 191: 6425-6435
Google Scholar: [Author Only](#) [Title Only](#) [Author and Title](#)
- Boehm M, Romero E, Reisinger V, Yu J, Komenda J, Eichacker LA, Dekker JP, Nixon PJ (2011) Investigating the early stages of Photosystem II assembly in *Synechocystis* sp. PCC 6803 isolation of CP47 and CP43 complexes. *J Biol Chem* 286: 14812-14819
Google Scholar: [Author Only](#) [Title Only](#) [Author and Title](#)
- Boehm M, Yu J, Reisinger V, Bečková M, Eichacker LA, Schlodder E, Komenda J, Nixon PJ (2012) Subunit composition of CP43-less photosystem II complexes of *Synechocystis* sp. PCC 6803: implications for the assembly and repair of photosystem II. *Philos Trans R Soc Ser B: Biol Sci* 367: 3444-3454
Google Scholar: [Author Only](#) [Title Only](#) [Author and Title](#)
- Bučinská L, Kiss E, Koník P, Knoppová J, Komenda J, Sobotka R (2018) The ribosome-bound protein Pam68 promotes insertion of chlorophyll into the CP47 subunit of photosystem II. *Plant Physiol* 176: 2931-2942
Google Scholar: [Author Only](#) [Title Only](#) [Author and Title](#)
- Chidgey JW, Linhartová M, Komenda J, Jackson PJ, Dickman MJ, Canniffe DP, Koník P, Pilný J, Hunter CN, Sobotka R (2014) A cyanobacterial chlorophyll synthase-HliD complex associates with the Ycf39 protein and the YidC/Alb3 insertase. *Plant Cell* 26: 1267-1279
Google Scholar: [Author Only](#) [Title Only](#) [Author and Title](#)
- Cormann KU, Bartsch M, Rögner M, Nowaczyk MM (2014) Localization of the CyanoP binding site on photosystem II by surface plasmon resonance spectroscopy. *Front Plant Sci* 5
Google Scholar: [Author Only](#) [Title Only](#) [Author and Title](#)
- Diner BA, Rappaport F (2002) Structure, dynamics, and energetics of the primary photochemistry of photosystem II of oxygenic photosynthesis. *Ann Rev Plant Biol* 53: 551-580
Google Scholar: [Author Only](#) [Title Only](#) [Author and Title](#)
- Dobáková M, Sobotka R, Tichý M, Komenda J (2009) Psb28 protein is involved in the biogenesis of the photosystem II inner antenna CP47 (PsbB) in the cyanobacterium *Synechocystis* sp. PCC 6803. *Plant Physiol* 149: 1076-1086
Google Scholar: [Author Only](#) [Title Only](#) [Author and Title](#)
- Dobáková M, Tichý M, Komenda J (2007) Role of the PsbI protein in photosystem II assembly and repair in the cyanobacterium *Synechocystis* sp PCC 6803. *Plant Physiol* 145: 1681-1691
Google Scholar: [Author Only](#) [Title Only](#) [Author and Title](#)
- Eaton-Rye JJ, Vermaas WF (1991) Oligonucleotide-directed mutagenesis of psbB, the gene encoding CP47, employing a deletion mutant strain of the cyanobacterium *Synechocystis* sp. PCC 6803. *Plant Mol Biol* 17: 1165-1177
Google Scholar: [Author Only](#) [Title Only](#) [Author and Title](#)
- García-Cerdán JG, Furst AL, McDonald KL, Schünemann D, Francis MB, Niyogi KK (2019) A thylakoid membrane-bound and redox-active rubredoxin (RBD1) functions in de novo assembly and repair of photosystem II. *Proc Natl Acad Sci USA* 116: 16631-16640
Google Scholar: [Author Only](#) [Title Only](#) [Author and Title](#)
- Giorgi LB, Nixon PJ, Merry SAP, Joseph DM, Durrant JR, Rivas JDL, Barber J, Porter G, Klug DR (1996) Comparison of primary charge separation in the photosystem II reaction center complex isolated from wild-type and D1-130 mutants of the cyanobacterium *Synechocystis* PCC 6803. *J Biol Chem* 271: 2093-2101
Google Scholar: [Author Only](#) [Title Only](#) [Author and Title](#)
- Gisriel CJ, Zhou KF, Huang HL, Debus RJ, Xiong Y, Brudvig GW (2020) Cryo-EM structure of monomeric photosystem II from *Synechocystis* sp. PCC 6803 lacking the water-oxidation complex. *Joule* 4: 2131-2148
Google Scholar: [Author Only](#) [Title Only](#) [Author and Title](#)
- Gounaris K, Chapman DJ, Barber J (1989) Isolation and characterisation of a D1/D2/cytochrome b-559 complex from *Synechocystis* 6803. *Biochim Biophys Acta* 973: 296-301
Google Scholar: [Author Only](#) [Title Only](#) [Author and Title](#)

- Gounaris K, Chapman DJ, Booth P, Crystall B, Giorgi LB, Klug DR, Porter G, Barber J (1990) Comparison of the D1/D2/cytochrome-b559 reaction center complex of photosystem two isolated by two different methods. *FEBS Lett* 265: 88-92
Google Scholar: [Author Only](#) [Title Only](#) [Author and Title](#)
- Guskov A, Kern J, Gabdulkhakov A, Broser M, Zouni A, Saenger W (2009) Cyanobacterial photosystem II at 2.9-Å resolution and the role of quinones, lipids, channels and chloride. *Nat Struct Mol Biol* 16: 334-342
Google Scholar: [Author Only](#) [Title Only](#) [Author and Title](#)
- Heinz S, Liauw P, Nickelsen J, Nowaczyk M (2016) Analysis of photosystem II biogenesis in cyanobacteria. *Biochim Biophys Acta* 1857: 274-287
Google Scholar: [Author Only](#) [Title Only](#) [Author and Title](#)
- Hey D, Grimm B (2018) ONE-HELIX PROTEIN2 (OHP2) is required for the stability of OHP1 and assembly factor HCF244 and is functionally linked to PSII biogenesis. *Plant Physiol* 177: 1453-1472
Google Scholar: [Author Only](#) [Title Only](#) [Author and Title](#)
- Hollingshead S, Kopečná J, Armstrong DR, Bučinská L, Jackson PJ, Chen GE, Dickman MJ, Williamson MP, Sobotka R, Hunter CN (2016) Synthesis of chlorophyll-binding proteins in a fully segregated $\Delta ycf54$ strain of the cyanobacterium *Synechocystis* PCC 6803. *Front Plant Sci* 7
Google Scholar: [Author Only](#) [Title Only](#) [Author and Title](#)
- Hollingshead S, Kopečná J, Jackson PJ, Canniffe DP, Davison PA, Dickman MJ, Sobotka R, Hunter CN (2012) Conserved chloroplast open-reading frame *ycf54* is required for activity of the magnesium protoporphyrin monomethylester oxidative cyclase in *Synechocystis* PCC 6803. *J Biol Chem* 287: 27823-27833
Google Scholar: [Author Only](#) [Title Only](#) [Author and Title](#)
- Ifuku K (2015) Localization and functional characterization of the extrinsic subunits of photosystem II: an update. *Biosc, Biotechnol, Biochem* 79: 1223-1231
Google Scholar: [Author Only](#) [Title Only](#) [Author and Title](#)
- Janouškovec J, Sobotka R, Lai DH, Flegontov P, Koník P, Komenda J, Ali S, Prášil O, Pain A, Oborník M, et al. (2013) Split photosystem protein, linear-mapping topology, and growth of structural complexity in the plastid genome of *Chromera velia*. *Mol Biol Evol* 30: 2447-2462
Google Scholar: [Author Only](#) [Title Only](#) [Author and Title](#)
- Kato K, Miyazaki N, Hamaguchi T, Nakajima Y, Akita F, Yonekura K, Shen J-R (2021) High-resolution cryo-EM structure of photosystem II reveals damage from high-dose electron beams. *Commun Biol* 4: 382
Google Scholar: [Author Only](#) [Title Only](#) [Author and Title](#)
- Kavanagh K, Jornvall H, Persson B, Oppermann U (2008) The SDR superfamily: functional and structural diversity within a family of metabolic and regulatory enzymes. *Cell Mol Life Sci* 65: 3895-3906
Google Scholar: [Author Only](#) [Title Only](#) [Author and Title](#)
- Kiss E, Knoppová J, Aznar GP, Pilný J, Yu J, Halada P, Nixon PJ, Sobotka R, Komenda J (2019) A photosynthesis-specific rubredoxin-like protein is required for efficient association of the D1 and D2 proteins during the initial steps of photosystem II assembly. *Plant Cell* 31: 2241-2258
Google Scholar: [Author Only](#) [Title Only](#) [Author and Title](#)
- Knoppová J, Sobotka R, Tichý M, Yu J, Koník P, Halada P, Nixon PJ, Komenda J (2014) Discovery of a chlorophyll binding protein complex involved in the early steps of photosystem II assembly in *Synechocystis*. *Plant Cell* 26: 1200-1212
Google Scholar: [Author Only](#) [Title Only](#) [Author and Title](#)
- Knoppová J, Yu JF, Janouškovec J, Halada P, Nixon PJ, Whitelegge JP, Komenda J (2021) The photosystem II assembly factor *Ycf48* from the cyanobacterium *Synechocystis* sp. PCC 6803 is lipidated using an atypical lipobox sequence. *Int J Mol Sci* 22
Google Scholar: [Author Only](#) [Title Only](#) [Author and Title](#)
- Knoppová J, Yu JF, Koník P, Nixon PJ, Komenda J (2016) CyanoP is involved in the early steps of photosystem II assembly in the cyanobacterium *Synechocystis* sp PCC 6803. *Plant Cell Physiol* 57: 1921-1931
Google Scholar: [Author Only](#) [Title Only](#) [Author and Title](#)
- Komenda J, Barker M, Kuviková S, de Vries R, Mullineaux CW, Tichý M, Nixon PJ (2006) The FtsH protease *slr0228* is important for quality control of photosystem II in the thylakoid membrane of *Synechocystis* sp PCC 6803. *J Biol Chem* 281: 1145-1151
Google Scholar: [Author Only](#) [Title Only](#) [Author and Title](#)
- Komenda J, Knoppová J, Kopečná J, Sobotka R, Halada P, Yu JF, Nickelsen J, Boehm M, Nixon PJ (2012a) The *Psb27* assembly factor binds to the CP43 complex of photosystem II in the cyanobacterium *Synechocystis* sp. PCC 6803. *Plant Physiol* 158: 476-486
Google Scholar: [Author Only](#) [Title Only](#) [Author and Title](#)
- Komenda J, Knoppová J, Krynická V, Nixon PJ, Tichý M (2010) Role of FtsH2 in the repair of photosystem II in mutants of the cyanobacterium *Synechocystis* PCC 6803 with impaired assembly or stability of the CaMn4 cluster. *Biochim Biophys Acta* 1797:

566-575

Google Scholar: [Author Only](#) [Title Only](#) [Author and Title](#)

Komenda J, Nickelsen J, Tichý M, Prášil O, Eichacker LA, Nixon PJ (2008) The cyanobacterial homologue of HCF136/YCF48 is a component of an early photosystem II assembly complex and is important for both the efficient assembly and repair of photosystem II in *Synechocystis* sp PCC 6803. *J Biol Chem* 283: 22390-22399

Google Scholar: [Author Only](#) [Title Only](#) [Author and Title](#)

Komenda J, Reisinger V, Muller BC, Dobáková M, Granvogl B, Eichacker LA (2004) Accumulation of the D2 protein is a key regulatory step for assembly of the photosystem II reaction center complex in *Synechocystis* PCC 6803. *J Biol Chem* 279: 48620-48629

Google Scholar: [Author Only](#) [Title Only](#) [Author and Title](#)

Komenda J, Sobotka R (2016) Cyanobacterial high-light-inducible proteins - Protectors of chlorophyll-protein synthesis and assembly. *Biochim Biophys Acta* 1857: 288-295

Google Scholar: [Author Only](#) [Title Only](#) [Author and Title](#)

Komenda J, Sobotka R, Nixon PJ (2012b) Assembling and maintaining the photosystem II complex in chloroplasts and cyanobacteria. *Curr Opin Plant Biol* 15: 245-251

Google Scholar: [Author Only](#) [Title Only](#) [Author and Title](#)

Kopečná J, Komenda J, Bučinská L, Sobotka R (2012) Long-term acclimation of the cyanobacterium *Synechocystis* sp. PCC 6803 to high light is accompanied by an enhanced production of chlorophyll that is preferentially channeled to trimeric photosystem I. *Plant Physiol* 160: 2239-2250

Google Scholar: [Author Only](#) [Title Only](#) [Author and Title](#)

Koskela MM, Skotnicová P, Kiss É, Sobotka R (2020) Purification of protein-complexes from the cyanobacterium *Synechocystis* sp. PCC 6803 using FLAG-affinity chromatography. *Bio-protocol* 10: e3616

Google Scholar: [Author Only](#) [Title Only](#) [Author and Title](#)

Krynická V, Shao S, Nixon PJ, Komenda J (2015) Accessibility controls selective degradation of photosystem II subunits by FtsH protease. *Nature Plants* 1: 15168

Google Scholar: [Author Only](#) [Title Only](#) [Author and Title](#)

Link S, Meierhoff K, Westhoff P (2012) The atypical short-chain dehydrogenases HCF173 and HCF244 are jointly involved in translational initiation of the *psbA* mRNA of *Arabidopsis thaliana*. *Plant Physiol*: pp.112.205104

Google Scholar: [Author Only](#) [Title Only](#) [Author and Title](#)

Lopez D, Koch G (2017) Exploring functional membrane microdomains in bacteria: an overview. *Cur Opin Microbiol* 36: 76-84

Google Scholar: [Author Only](#) [Title Only](#) [Author and Title](#)

Lu Y (2016) Identification and roles of photosystem II assembly, stability, and repair factors in *Arabidopsis*. *Front Plant Sci* 7

Google Scholar: [Author Only](#) [Title Only](#) [Author and Title](#)

Malavath T, Caspy I, Netzer-EI SY, Klaiman D, Nelson N (2018) Structure and function of wild-type and subunit-depleted photosystem I in *Synechocystis*. *Biochim Biophys Acta* 1859: 645-654

Google Scholar: [Author Only](#) [Title Only](#) [Author and Title](#)

Mayer SR, Dubbs JM, Vass I, Hideg E, Nagy L, Barber J (1993) Further characterization of the *psbH* locus of *Synechocystis* sp. PCC 6803: Inactivation of *psbH* impairs QA to QB electron transport in photosystem 2. *Biochemistry* 32: 1454-1465

Google Scholar: [Author Only](#) [Title Only](#) [Author and Title](#)

Muller B, Eichacker LA (1999) Assembly of the D1 precursor in monomeric photosystem II reaction center precomplexes precedes chlorophyll a-triggered accumulation of reaction center II in barley etioplasts. *Plant Cell* 11: 2365-2377

Google Scholar: [Author Only](#) [Title Only](#) [Author and Title](#)

Myouga F, Takahashi K, Tanaka R, Nagata N, Kiss AZ, Funk C, Nomura Y, Nakagami H, Jansson S, Shinozaki K (2018) Stable accumulation of photosystem II requires ONE-HELIX PROTEIN1 (OHP1) of the light harvesting-like family. *Plant Physiol* 176: 2277-2291

Google Scholar: [Author Only](#) [Title Only](#) [Author and Title](#)

Nanba O, Satoh K (1987) Isolation of a photosystem-II reaction center consisting of D-1 and D-2 polypeptides and cytochrome-b-559. *Proc Natl Acad Sci USA* 84: 109-112

Google Scholar: [Author Only](#) [Title Only](#) [Author and Title](#)

Nickelsen J, Rengstl B (2013) Photosystem II assembly: from cyanobacteria to plants. In SS Merchant, ed, *Ann Rev Plant Biol*, Vol 64, pp 609-635

Google Scholar: [Author Only](#) [Title Only](#) [Author and Title](#)

Nixon PJ, Michoux F, Yu JF, Boehm M, Komenda J (2010) Recent advances in understanding the assembly and repair of

photosystem II. *Ann Bot* 106: 1-16

Google Scholar: [Author Only](#) [Title Only](#) [Author and Title](#)

Oren-Shamir M, Sai PSM, Edelman M, Scherz A (1995) Isolation and spectroscopic characterization of a plant-like photosystem-II reaction center from the cyanobacterium *Synechocystis* sp. 6803. *Biochemistry* 34: 5523-5526

Google Scholar: [Author Only](#) [Title Only](#) [Author and Title](#)

Pakrasi HB, Williams JGK, Arntzen CJ (1988) Targeted mutagenesis of the *psbE* and *psbF* genes blocks photosynthetic electron transport: evidence for a functional role of cytochrome *b559* in photosystem II. *EMBO J* 7: 325-332

Google Scholar: [Author Only](#) [Title Only](#) [Author and Title](#)

Rast A, Schaffer M, Albert S, Wan W, Pfeffer S, Beck F, Plietzko JM, Nickelsen J, Engel BD (2019) Biogenic regions of cyanobacterial thylakoids form contact sites with the plasma membrane. *Nat Plants* 5: 436-446

Google Scholar: [Author Only](#) [Title Only](#) [Author and Title](#)

Ritchie RJ (2006) Consistent sets of spectrophotometric chlorophyll equations for acetone, methanol and ethanol solvents. *Photosynthesis Res* 89: 27-41

Google Scholar: [Author Only](#) [Title Only](#) [Author and Title](#)

Rivera-Milla E, Stuermer CAO, Malaga-Trillo E (2006) Ancient origin of reggie (flotillin), reggie-like, and other lipid-raft proteins: convergent evolution of the SPFH domain. *Cel Mol Life Sci* 63: 343-357

Google Scholar: [Author Only](#) [Title Only](#) [Author and Title](#)

Romero E, Diner Bruce A, Nixon Peter J, Coleman William J, Dekker Jan P, van Grondelle R (2012) Mixed exciton-charge-transfer states in photosystem II: Stark spectroscopy on site-directed mutants. *Biophys J* 103: 185-194

Google Scholar: [Author Only](#) [Title Only](#) [Author and Title](#)

Roose JL, Frankel LK, Mummadisetti MP, Bricker TM (2016) The extrinsic proteins of photosystem II: update. *Planta* 243: 889-908

Google Scholar: [Author Only](#) [Title Only](#) [Author and Title](#)

Saikawa N, Akiyama Y, Ito K (2004) FtsH exists as an exceptionally large complex containing HflKC in the plasma membrane of *Escherichia coli*. *J Struct Biol* 146: 123-129

Google Scholar: [Author Only](#) [Title Only](#) [Author and Title](#)

Schottkowski M, Gkalymoudis S, Tzekova N, Stelljes C, Schunemann D, Ankele E, Nickelsen J (2009) Interaction of the periplasmic PrtA factor and the PsbA (D1) protein during biogenesis of photosystem II in *Synechocystis* sp PCC 6803. *J Biol Chem* 284: 1813-1819

Google Scholar: [Author Only](#) [Title Only](#) [Author and Title](#)

Shen GZ, Boussiba S, Vermaas WFJ (1993) *Synechocystis* sp PCC-6803 strains lacking Photosystem-I and phycobilisome function. *Plant Cell* 5: 1853-1863

Google Scholar: [Author Only](#) [Title Only](#) [Author and Title](#)

Shinopoulos KE, Brudvig GW (2012) Cytochrome *b559* and cyclic electron transfer within photosystem II. *Biochim Biophys Acta* 1817: 66-75

Google Scholar: [Author Only](#) [Title Only](#) [Author and Title](#)

Shukla MK, Llansola-Portoles MJ, Tichý M, Pascal AA, Robert B, Sobotka R (2018) Binding of pigments to the cyanobacterial high-light-inducible protein HliC. *Photosynthesis Res* 137: 29-39

Google Scholar: [Author Only](#) [Title Only](#) [Author and Title](#)

Staleva H, Komenda J, Shukla MK, Šlouf V, Kaňa R, Polívka T, Sobotka R (2015) Mechanism of photoprotection in the cyanobacterial ancestor of plant antenna proteins. *Nat Chem Biol* 11: 287-291

Google Scholar: [Author Only](#) [Title Only](#) [Author and Title](#)

Suzuki H, Yu JF, Kobayashi T, Nakanishi H, Nixon PJ, Noguchi T (2013) Functional roles of D2-Lys317 and the interacting chloride ion in the water oxidation reaction of photosystem II as revealed by Fourier transform infrared analysis. *Biochemistry* 52: 4748-4757

Google Scholar: [Author Only](#) [Title Only](#) [Author and Title](#)

Tang XS, Chisholm DA, Dismukes GC, Brudvig GW, Diner BA (1993) Spectroscopic Evidence from Site-Directed Mutants of *Synechocystis* PCC6803 in Favor of a Close Interaction between Histidine-189 and Redox-Active Tyrosine-1608 Both of Polypeptide D2 of the Photosystem II Reaction Center. *Biochemistry* 32: 13742-13748

Google Scholar: [Author Only](#) [Title Only](#) [Author and Title](#)

Thompson EP (2016) Proteins involved in the maintenance of the photosynthetic apparatus in cyanobacteria and plants. Ph.D. thesis. University College London

Google Scholar: [Author Only](#) [Title Only](#) [Author and Title](#)

Tomo T, Akimoto S, Tsuchiya T, Fukuya M, Tanaka K, Mimuro M (2008) Isolation and spectral characterization of photosystem II

reaction center from *Synechocystis* sp PCC 6803. *Photosynthesis Res* 98: 293-302

Google Scholar: [Author Only](#) [Title Only](#) [Author and Title](#)

Torabi S, Umate P, Manavski N, Plochinger M, Kleinknecht L, Bogireddi H, Herrmann RG, Wanner G, Schroder WP, Meurer J (2014) PsbN is required for assembly of the photosystem II reaction center in *Nicotiana tabacum*. *Plant Cell* 26: 1183-1199

Google Scholar: [Author Only](#) [Title Only](#) [Author and Title](#)

Trinugroho JP, Bečková M, Shao S, Yu J, Zhao Z, Murray JW, Sobotka R, Komenda J, Nixon PJ (2020) Chlorophyll f synthesis by a super-rogue photosystem II complex. *Nature Plants* 6: 238-244

Google Scholar: [Author Only](#) [Title Only](#) [Author and Title](#)

Umena Y, Kawakami K, Shen JR, Kamiya N (2011) Crystal structure of oxygen-evolving Photosystem II at a resolution of 1.9 Å. *Nature* 473: 55-60

Google Scholar: [Author Only](#) [Title Only](#) [Author and Title](#)

Vácha F, Durchan M, Siffel P (2002) Excitonic interactions in the reaction centre of photosystem II studied by using circular dichroism. *Biochim Biophys Acta* 1554: 147-152

Google Scholar: [Author Only](#) [Title Only](#) [Author and Title](#)

Walters RG, Shephard F, Rogers JJM, Rolfe SA, Horton P (2003) Identification of mutants of *Arabidopsis* defective in acclimation of photosynthesis to the light environment. *Plant Physiol* 131: 472-481

Google Scholar: [Author Only](#) [Title Only](#) [Author and Title](#)

Xu Q, Bateman A, Finn RD, Abdubek P, Astakhova T, Axelrod HL, Bakolitsa C, Carlton D, Chen C, Chiu H-J, et al. (2010) Bacterial pleckstrin homology domains: A prokaryotic origin for the PH domain. *J Mol Biol* 396: 31-46

Google Scholar: [Author Only](#) [Title Only](#) [Author and Title](#)

Yu JF, Knoppová J, Michoux F, Bialek W, Cota E, Shukla MK, Strašková A, Aznar GP, Sobotka R, Komenda J, et al. (2018) Ycf48 involved in the biogenesis of the oxygen-evolving photosystem II complex is a seven-bladed beta-propeller protein. *Proc Natl Acad Sci USA* 115: E7824-E7833

Google Scholar: [Author Only](#) [Title Only](#) [Author and Title](#)

Zouni A, Witt HT, Kern J, Fromme P, Krauss N, Saenger W, Orth P (2001) Crystal structure of photosystem II from *Synechococcus elongatus* at 3.8 Å resolution. *Nature* 409: 739-743

Google Scholar: [Author Only](#) [Title Only](#) [Author and Title](#)